EALG-21012

JJ-FAST Technical Note

Ver. 11 (April 27, 2026)

Japan International Cooperation Agency (JICA)

Japan Aerospace Exploration Agency (JAXA)

Table of Contents

1. System Overview

The New JICA-JAXA Forest Early Warning System in the Tropics (JJ-FAST) employs JAXA's next-generation deforestation detection algorithm to spot deforestation areas with size larger than 1.5 hectares (Ver. 4.0, as of April 2023). Exploiting Japan's state-of-the-art radar Earth observation (EO) technology together with powerful next-generation algorithms, detections can be made even under the thick cloud cover which is characteristic for tropical regions especially during the rainy seasons. Most importantly, as the New JJ-FAST aims to finally function as a veritable Early Warning System, the new algorithms focus on detection only fresh and ongoing deforestation activities. Reliable deforestation polygons will be published online on the JJ-FAST website only 3 days after the ALOS-2 image acquisition giving local authorities enough time to take meaningful actions.

The system detects deforestation by means of L-band (1.25 MHz) Synthetic Aperture Radar (SAR) data acquired by the PALSAR-2 sensor aboard JAXA's Advanced Land Observing Satellite 2 (ALOS-2) and provides geolocated polygons for every detected site free of charge via its web service. To achieve full areal coverage of the entire tropical forest belt, ALOS-2 operated in ScanSAR mode which has a 350-km swath at the cost of reduced image resolution. The ALOS-2 JJ-FAST image data comes at a natural resolution of 50-m. Hence, the potential to track very small-scale deforestation is limited by the coarse spatial resolution. With unique Early Warning capabilities and frequent updates, approximately every 1.5 months, JJ-FAST can serve as an effective deterrent against illegal deforestation activities when forest authorities in the target countries act accordingly on the JJ-FAST alerts. Government forest authorities of tropical countries with large forest inventories are targeted as the main users of JJ-FAST. Since the Early Warning polygons of detected deforestations cannot only be conveniently viewed online, but also downloaded for further GIS analysis, local authorities are able to effectively identify illegal activities by comparing JJ-FAST detections with available national land use maps and/or concession maps. The target region of JJ-FAST includes 78 countries (Fig. 1, Tab. 1), covering almost the entire tropical forest belt until March 2024. Since April 2024, JJ-FAST updates have been limited to Brazil.

Fig. 1 The 78 JJ-FAST target countries in the tropical belt until March 2024.

Table 1 List of JJ-FAST target countries by regions until March 2024.

Region	Country
South America	Bolivia, Brazil, Colombia, Ecuador, Guyana, Paraguay, Peru, Suriname, Venezuela
Central America	Belize, Costa Rica, El Salvador, Guatemala, Honduras, Mexico, Nicaragua, Panama, Trinidad and Tobago
Africa	Benin, Burkina Faso, Cote d'Ivoire, Ghana, Guinea, Guinea-Bissau, Liberia, Mali,

	Nigeria, Senegal, Sierra Leone, Togo, Burundi, Djibouti, Ethiopia, Kenya, Rwanda, Seychelles, Somalia, Sudan, South Sudan, Tanzania, Uganda, Cameroon, Central African Republic, Chad, Republic of Congo, Democratic Republic of Congo, Equatorial Guinea, Gabon, Madagascar, Angola, Botswana, Lesotho, Malawi, Mauritius, Mozambique, Namibia, Republic of South Africa, Sao Tome and Principe, Swaziland, Zambia, Zimbabwe
Asia	Bangladesh, Bhutan, Brunei, Cambodia, India, Indonesia, Laos, Malaysia, Myanmar, Nepal, Philippines, Sri Lanka, Thailand, Timor-Leste, Viet Nam
Oceania	Papua New Guinea, Solomon Islands

2. JJ-FAST Product Description

JJ-FAST does not only allow to view Early Warning polygons online on the interactive map, but all the deforestation polygons can be downloaded by users in units of 1°×1° tiles. The download file can be selected from two types of formats: ESRI Shape format or KML format. The file naming convention is explained in Figure 2. Most importantly users should note that the date of detection is provided in the filename of every JJ-FAST product in for of 6 digits (YYMMDD) date forma. The second date indicates the last observation prior the detection. The attribute information shown in Figure 3 is attached to each polygon. WGS84 is used as a geodetic system in the geographic coordinate system (latitude and longitude coordinates).

JJ-FAST early warning polygon attributes are summarized in Table 2. Note that the attribute information for Ver. 4.0 is different from this, as shown in Table 3.

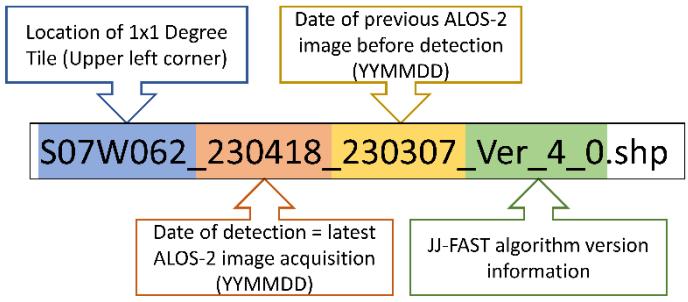

Fig. 2 Description of the JJ-FAST product file name convention.

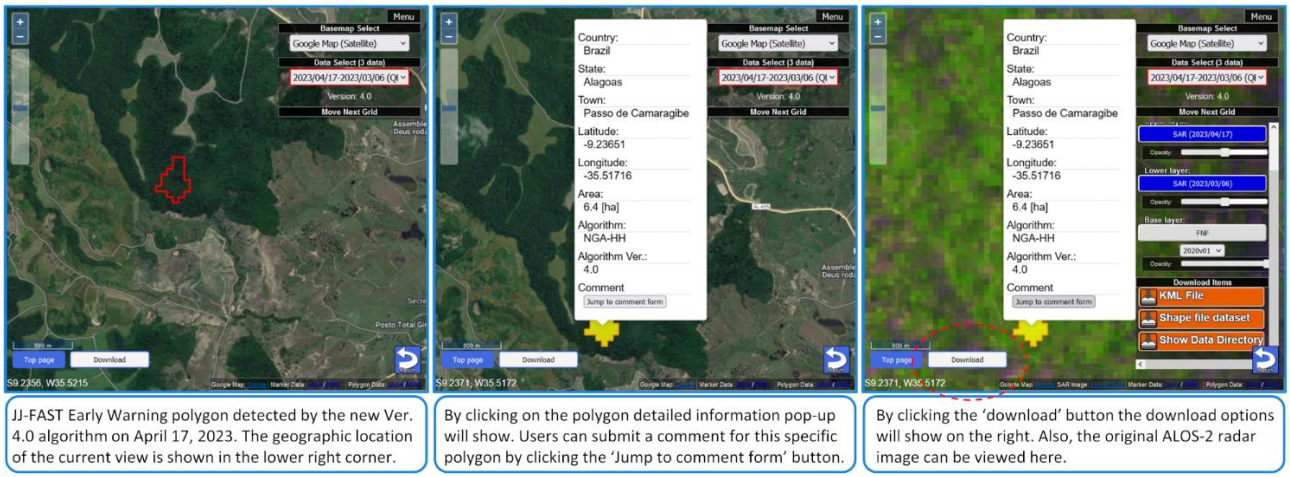

Fig. 3 Example of JJ-FAST Website display with attributes of the New Ver. 4.0.

Table 2 Attribute information of the deforestation polygon.

Field name	Pop-up name	Contents
Country	Country	Country name where the polygon center is located
Continent	-	Continent name where the polygon center is located
ChangeArea	Change Area	Area of polygon (in hectares)
Accuracy	Reliability	Reliability of detection results (for Ver. 3.2): 1 = high reliability (the change of PALSAR-2 images exceeds the threshold of Table A3 by 1.0 dB) 2 = medium reliability (the change exceeds the threshold)
Polygon_id	-	ID for identifying each polygon
State	State	State name where the polygon center is located
Town	Town	Town name where the polygon center is located
Latitude	Latitude	Latitude of the polygon center
Longitude	Longitude	Longitude of the polygon center
Algorithm	Algorithm	Methodology of deforestation detection
AlgoVer	Algorithm Ver.	Version of algorithm
Threshold	Threshold	Threshold area defined for version-3 algorithm

Table 3 Attribute information of the deforestation polygon of the New Ver. 4.0.

Field name	Pop-up name	Contents
Polygon_ID	Country	Unique identifier for each Early Warning polygon
Latitude	Lat	Latitude of the polygon center in decimal degree
Longitude	Lon	Longitude of the polygon center in decimal degree
Area	Area [ha]	Size of deforested area in hectares
Algorithm	Algorithm	Name of the next-generation algorithm (NGA)
Algorithm Ver.	Version	JJ-FAST version

Country	Country	Country name where the polygon is located
State	State	State name where the polygon is located
Town	Town	Town name where the polygon is located

Every downloaded JJ-FAST polygon shapefile is accompanied by a system control file in the form of a JavaScript Object Notation (JSON) file (file extension ".json"). In the JSON file, the source data and the polygon information are described with the key of "source_data" and "polygon_info" respectively. The "source_data" lists the information of time-series PALSAR-2 images processed for forest change detection and the "polygon_info" lists the polygon attributes for each polygon. The JSON data structure description can be found in Table 8A in the appendix.

3. ALOS-2 Time-Series Data Acquisition and ScanSAR Imaging Algorithms

The dual-polarization ScanSAR mode of ALOS-2 is used to observe the whole region in both HH and HV polarization with frequent revisits at least nine times per year. The ScanSAR mode covers a wide-area observation of 350 km swath by scanning five 70km-sub-swathes (for more information, see the web site: http://www.eorc.jaxa.jp/ALOS-2/en/about/palsar2.htm).

Most of the ScanSAR data, that are acquired following the ALOS-2 Basic Observation Scenario (BOS) and fully or partially cover the target region, are extracted from level 1.0 data and are long-strip imaged using the Sigma-SAR processor to prepare for the later time series datasets. Maximum imaging length sometime reaches up to 3,000 km. Time-varying SAR parameters are properly corrected and the uniform long-strip images are produced. To suppress the speckle noise, 4 range samples are averaged and 50-meter subsampling in azimuth are adopted. Specan algorithm was adopted for quicker processing and the scalloping minimization was conducted. After this, the ortho-rectification and slope correction (as the radiometric terrain correction) using the SRTM1-DEM, EGM96 geoid model, and GRS80 georeference system are performed. Finally, the data are projected onto the Equirectangular map at 50-m pixel spacing. Detailed processing algorithms are described in the following reference (Shimada, 2018). Radiometric and geometric calibrations were conducted using the known calibration sites.

A detailed overview of the PALSAR-2 data and the various ancillary data used in the JJ-FAST processing scheme is provided in Table A6 and Table A7, respectively, in the Appendix of this document.

4. Deforestation detection algorithm

The NEW JJ-FAST Ver. 4.0 employs the Next-Generation Algorithm (NGA) which finally achieves veritable Early Warning capability and unrivaled reliability. The extremely powerful and future proof NGA is a completely new development breaking with all prior, insufficient algorithm generations. It is expected that no major algorithm

changes will be required in the future.

Prior to the launch of the New JJ-FAST, five different algorithm versions for deforestation detection have been used (Table 4). The most current algorithm was Ver 3.2 as introduced in September 2022. This algorithm will be described in this section following the introduction of the next-generation algorithm that replaces all previous generations. Detailed description of the older discontinued algorithm versions 0.0 - 3.1 can be found in the appendix of this document. It should be pointed out that due to the insufficiency of previous JJ-FAST versions we do not recommend relying on detections made before September 2022 as the results were generally not very reliable.

Table 4 Revision history of the deforestation detection algorithm.

Algorithm version	Application period	Algorithm
Ver. 0.0	2016.11 – 2017.07	Change detection between 2 images of PALSAR-2 HV
Ver. 1.0	2017.07 – 2018.04	Change detection between 2 images of PALSAR-2 HV
Ver. 2.0	2018.04 – 2018.07	Analysis using a reference from 10 scenes of PALSAR-2 HV, HH
Ver. 2.0	2018.07 – 2019.06	Analysis using a reference from 15 scenes of PALSAR-2 HV, HH
Ver. 2.1	2019.07 – 2020.05	Analysis using a reference from 20 scenes of PALSAR-2 HV, HH with updated thresholds
Ver. 3.0	2020.06 – 2022.03	Data process unit changes from polygon to pixel base. Applying temporal normalization Introducing different threshold level depending on the site.
Ver. 3.1[1)]	2022.03 – 2022.09	Applying advanced false-alarm suppression based on new pixel-based full time-series analysis. Introduction of new PALSAR-2 ScanSAR time-series forest/non-forest (TS-FNF) mask
Ver. 3.2	2022.09 – 2023.04	The advanced false-alarm suppression and the new PALSAR-2 ScanSAR TS-FNF mask, introduced in Latin America in Ver. 3.1, are now used in the entire JJ-FAST area. The 'Sigma-SAR' ScanSAR processor was upgraded from v2.4.0 to v3.0.0.
Ver. 4.0	2023.04 –2023.11	The NEW JJ-FAST employs the Next-Generation Algorithm (NGA) which finally achieves veritable Early Warning capability and unrivaled reliability. The powerful and future proof NGA is a completely new development breaking with all prior algorithm generations.
Ver. 4.1	2023.11 –2026.04	The parametrization of the new Ealy Warning algorithm was improved based on field survey data and the comprehensive validation data from the three validation supersites in Brazil. A new HV change detection algorithm was introduced to enable detections of deforestation cases which are not suitable for Early Warning detection.
Ver. 4.2	2026.04 –	The processing resolution was refined from a 1°×1° grid to a 0.1°×0.1° grid. Computing all time-series parameters at 100 times higher resolution greatly enhanced robustness under difficult environmental conditions, e.g., localized heavy rainfall and severe local flooding. The Degree of Polarization (DoP) was introduced as a new parameter to improve dynamic forest masking and forest loss detection.

[1)] Ver. 3.1 was used only in Latin America while Ver. 3.0 was used in Africa, Asia, and Oceania.

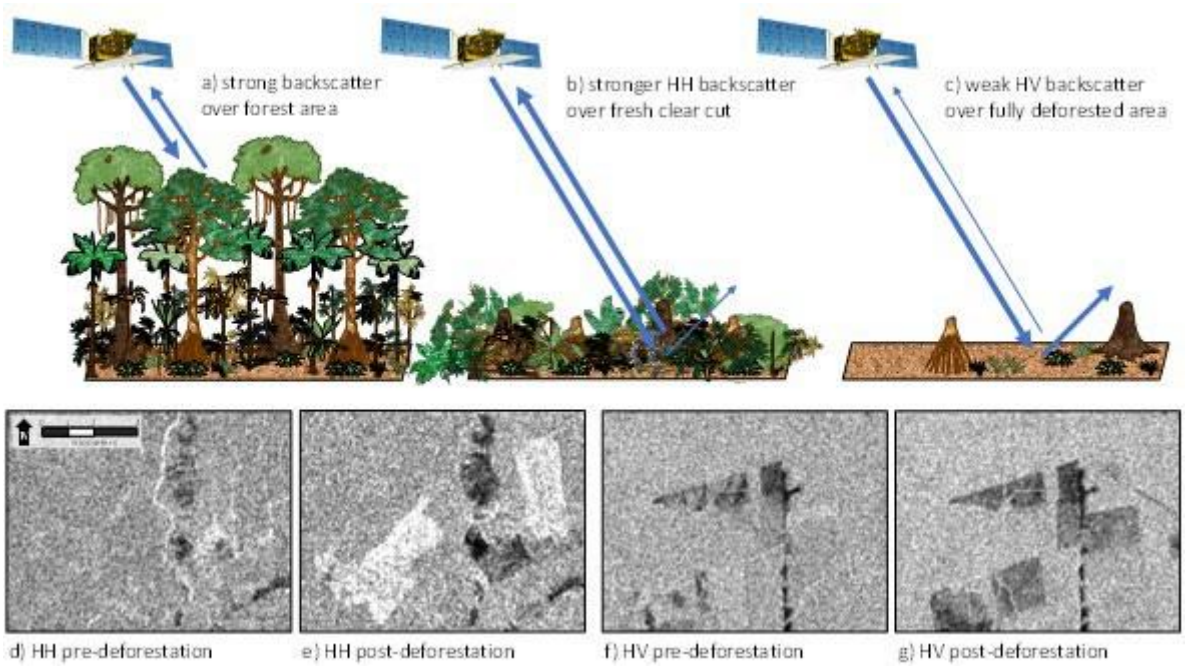

Fig. 4 Schematic of the deforestation detection principle by increasing HH backscatter (a, b, d, e) or decreasing HV backscatter (a, c, f, g).

■ Next-generation algorithm (JJ-FAST Ver. 4.0, Ver. 4.1, Ver. 4.2)

JAXA's next-generation algorithm (NGA) used in JJ-FAST 4.0 is a powerful fully integrated dual-polarization deforestation Early Warning algorithm. Thanks to tremendous improvements, the New JJ-FAST finally realizes the first veritable deforestation Early Warning System in the tropics. Unlike the previous change detection algorithm generations, the NGA gives priority to HH change detection in order to detect only fresh and ongoing deforestations. The unreliable and ambiguous detections with long delays, as was characteristic with the Old JJ-FAST, are a thing of the past. The process flow chart of the next-generation algorithm is shown in Figure 5. The most important new features are highlighted below.

- The New Algorithm exploits the full dual-polarization time-series information
  - Prioritizing HH for change detection, HV for non-forest masking
- Forest Mask (TS-FNF) and FloodMask (TS-Mask) are processed on the fly
  - Forest cover information is always up to date, eliminating non-forest errors
  - No auxiliary data apart DEM for SAR processing and masking of steep slopes are required
  - Eliminates uncertainties introduced by unreliable, outdated, unsuitable external information
- Fast processing speed
  - Reduces computational costs
- Set of 9 adjustable backscatter parameters plus 3 TS parameters

- Allows adaptions for wide variety of seasonal conditions, forest types, etc.

- Advanced forest backscatter statistics calculation
  - Allows automatic calibration for seasonal effects and local parameter adjustments.

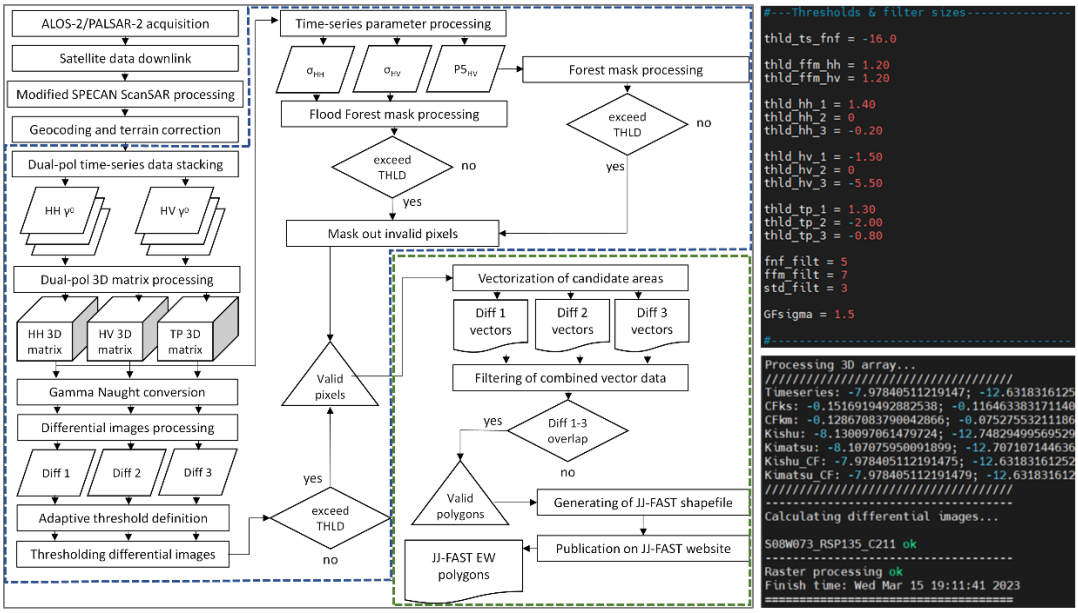

Fig. 5 Processing flow of the next-generation deforestation detection algorithm used in Ver. 4.0.

Thanks to highly sophisticated 3D time-series processing, the next-generation algorithm can now detect the size of a deforested area with great precision.

Note that the scientific research paper on the next-generation is currently being prepared for publication. The full details of this cutting-edge development will be disclosed in this Technical Note document after publication, and the research paper will be made available to download as well. An example of the outstanding performance of the New JJ-FAST is shown in Figure 6. The comparison with cloud-free optical Planet daily images, taken quasi-simultaneously with the ALOS-2 images, demonstrates the unmatched quality of the next-generation algorithm.

From C235, Ver. 4.0.2 introduced a new slope mask derived from the ALOS World 3D (AW3D30) DEM to reduce false alarms in mountainous areas with steep topography. The maximum slope angle in Ver. 4.0 is set to 15 degrees. In addition, the Global Human Settlement Layer is used to mask built-up areas where sometimes error detections occurred (see Table A7).

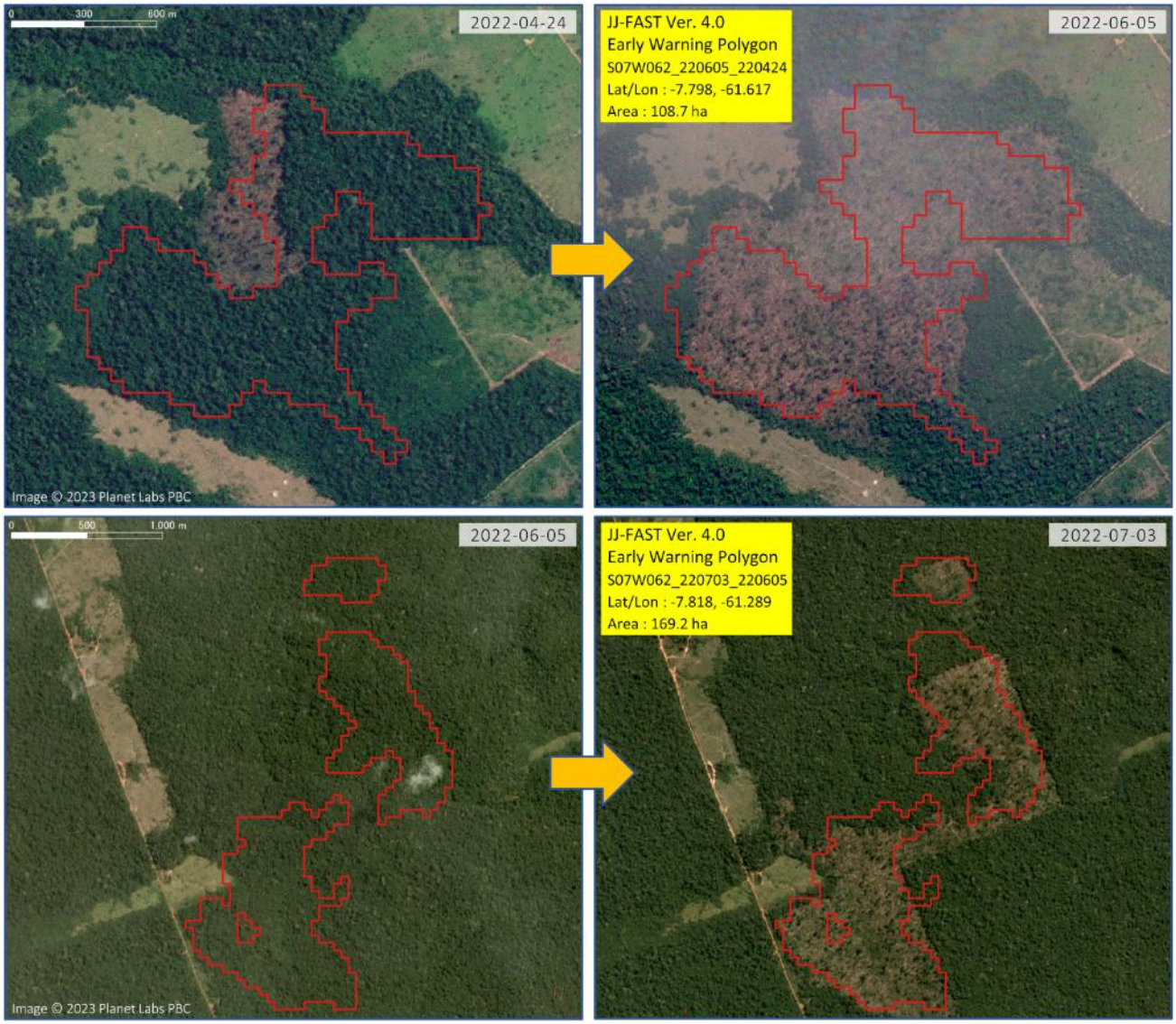

Fig. 6 Examples of Early Warning polygons detected by the New JJ-FAST at 2 sites in Amazonia, Brazil. The next generation algorithm detected fresh/ongoing deforestation activity at unprecedented precision. (Image © Planet Labs PBC)

■ Algorithm Ver. 4.1

Ver 4.1 was launched for C243 on October 31, 2023. The main modifications as compared to Ver. 4.0 comprise improvement of the flood false alarm suppression as well as improved parameterization of the area dependent change detection thresholds. These improvements are largely based on findings made during a joint field survey with IBAMA in the Rio Branco region, Brazil, as well as on the validation and calibration data available for three super sites in the Legal Amazon (see Section 5). After some consideration, Ver. 4.1 reintroduced an HV algorithm, as it was found that it can improve producer's accuracy in some cases. The new HV algorithm follows the well-known change detection principle that relates deforestation to a decrease in HV backscatter (Fig. 4). The advantage of the HV

algorithm is that it can detect very small forest cover changes with a minimum size of only 1 ha. However, it is important to note that in general Ver. 4.1 gives priority to the next-generation HH early warning algorithm. In most cases the HV algorithm in fact redetects deforestation areas that have previously already been detected by the HH early warning main algorithm as shown in Fig. 7.

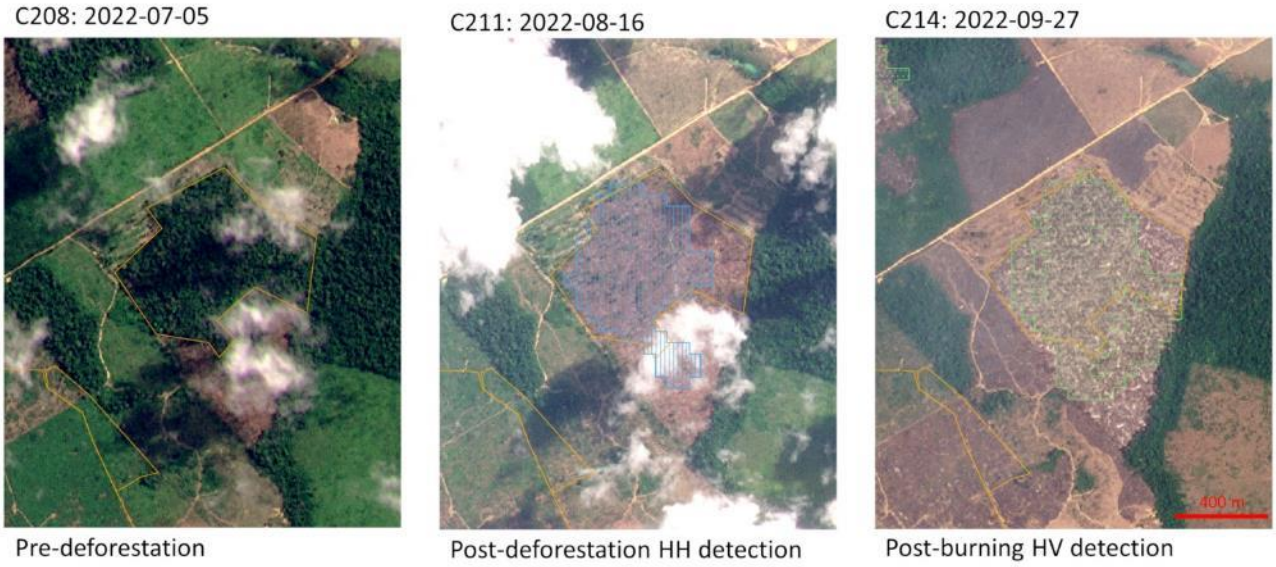

Fig. 7 Example of an Early Warning polygon detected by the Ver 4.1 HH algorithm and the redetection by the HV algorithm during the next observation cycle. (Image © Planet Labs PBC)

■ Algorithm Ver. 4.2

Ver 4.2 was launched with the start of ALOS-2 observation cycle C307 on April 13, 2026. The main improvement in Ver 4.2 over Ver 4.1 comes from grid refinement. In Ver 4.1, all time-series statistical parameters used for automatic threshold adjustment to environmental conditions at the latest (T0) observation were calculated over the full 1° × 1° tiles. In Ver 4.2, each tile is processed at a 0.1° × 0.1° subgrid, resulting in a 100-fold finer spatial resolution.

The coarse 1° × 1° resolution in Ver 4.1 caused issues under certain conditions, particularly heavy localized rainfall and isolated severe flood events along rivers, which affected only small subareas within a tile. The 100 times finer processing resolution in Ver 4.2 better accounts for small-scale spatio-temporal variability. Significant reduction of false alarms under these conditions has been confirmed.

Fig. 8 shows an example of the accuracy improvements achieved with Ver 4.2. The data were acquired over tile S09W063 at the beginning of the rainy season in November 2024. While Ver 4.1 detected 253 polygons in the area, Ver 4.2 detected only 67. As shown, the large number of false alarms in areas with significantly higher variability, caused by localized heavy rainfall and associated temporary surface flooding, were largely suppressed thanks to the finer grid resolution in Ver 4.2.

In this example, User's Accuracy increased substantially from 11.5% (Ver 4.1) to 62.7% (Ver 4.2). In addition,

Producer's Accuracy also improved, with Ver 4.2 detecting 42 true deforestation events compared to only 29 with Ver 4.1.

Furthermore, Ver 4.2 introduces the Degree of Polarization (DoP) as an additional time-series change detection parameter, enhancing the robustness of both dynamic forest masking and deforestation detection.

The highest false alarm rates in Ver 4.1 occurred under the aforementioned conditions. Validation using 3,052 fully inspected early warning polygons detected in 2024 (polygon sizes ranging from 1.5 ha to 320 ha) demonstrated an improvement in overall User's Accuracy of approximately 45% (from 49.7% in Ver 4.1 to 71.1% in Ver 4.2).

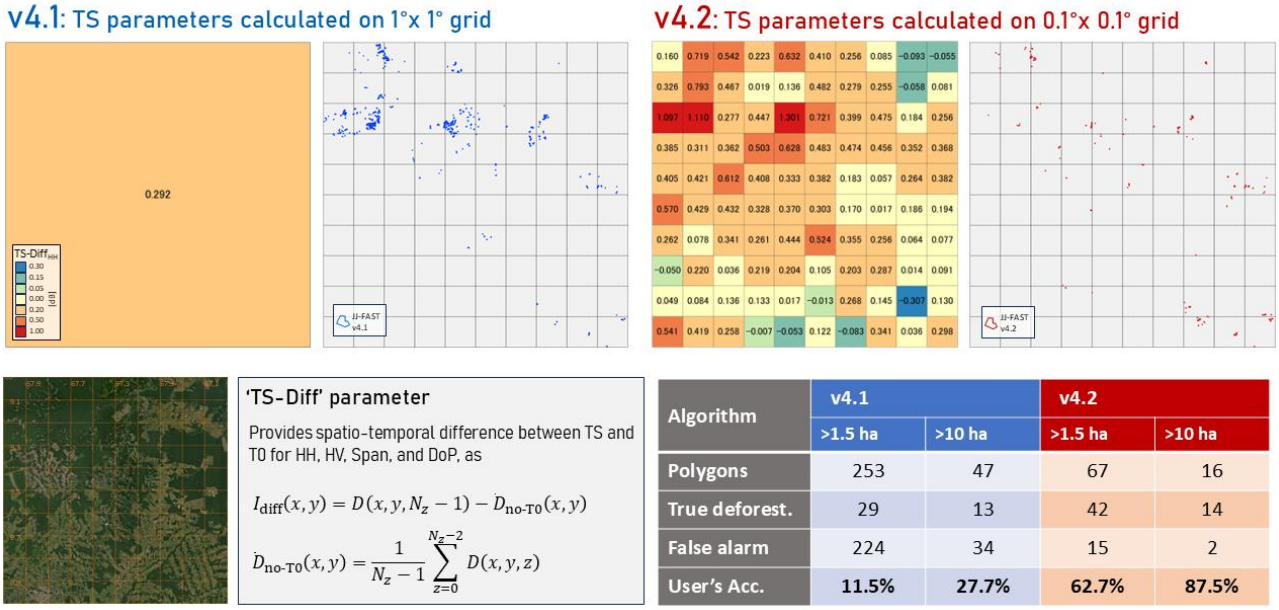

Algorithm	v4.1		v4.2	
	>1.5 ha	>10 ha	>1.5 ha	>10 ha
Polygons	253	47	67	16
True deforest.	29	13	42	14
False alarm	224	34	15	2
User's Acc.	11.5%	27.7%	62.7%	87.5%

Fig. 8 Example of operational accuracy improvement by v4.2 grid-refinement in tile S09W063 at the beginning of the rainy season in November 2024. Whilst v4.1 processed TS statistical parameters over the entire 1°x1° tile, v4.2 performs calculations at a 100-fold finer resolution, resulting in substantial reduction in false alarms and omission errors.

■ Algorithm Ver. 3.2 (discontinued)

Despite some improvements in the Ver. 3.0 algorithm, there were still several factors that drastically hampered the reliability of the produced forest warnings. Due to these prevailing issues with critically low deforestation detection accuracies of Ver. 3 algorithm, this update introduced a novel false alarm suppression method based on advanced time-series analysis using all available JJ-FAST PALSAR-2 ScanSAR data. Note that the basic change detection method for deforestation detection of Ver. 3 is unchanged. The processing flow for Ver 3.1 which is in use since March 7, 2022, is shown in Fig. 7. As most of the severely low accuracy results are related to flooding and rainfall effects, we propose a new full-resolution flood forest mask which can be used to filter out all false positives caused by heavy rain and flooding of forest floor. An example of such a flood forest map is shown in Fig. 8. The map is based on the

full ALOS-2 time-series using 73 cycles. It is the first time that such a reliable high-resolution and area-wide flood forest information has been used and it well demonstrates the tremendous potential of the unprecedented ALOS-2/PALSAR-2 long-term observation archive. The filtering of error polygons is done on the basis of a proposed omega parameter. This parameter is calculated for every QL polygon by using the information from the flood forest masks. Omega parameter is calculated using the mean temporal standard deviation of all ScanSAR image pixels inside a given polygon and the maximum temporal standard deviation out of all the pixels inside the polygon (Fig. 9) as

$$\omega = \frac{\frac{2}{s}(\sum_{i=1}^{s} x_i) + \max_{i\in[s]} x_i}{3}$$

where s is the number of pixels inside the detected polygon and x_i is the γ^0 standard deviation of pixel i.

It has been confirmed that the new method can reduce the number of false positives by up to 97.5% depending on the severity of the rainfall events and flooding conditions.

In addition, in Ver 3.1 we introduce a new PALSAR-2 ScanSAR time-series FNF mask to drastically reduce false detections related to incorrect landcover information. The new forest mask is also based on the ScanSAR full time-series analysis. In principle, the decision whether an image pixel is covered by forest or not is made based the 5th percentile (*P5*) of the γ^0_{HV} time-series (Fig. 10). If a pixel exceeds a threshold value (e.g., -16.5 dB in the case of Amazon basin) it is classified as forest, and if it is below that threshold it is classified as non-forest. The new approach has several main advantages over the old forest mask. First, the maps are self-updating with every new cycle, keeping them always up-to-date. Second, the masks are produced for every RPS path resulting in exactly matching image 12geometries. And lastly, the new maps are much more reliable than the older maps because the time-series approach largely reduces all uncertainties caused by spatial-temporal variability and seasonality effects which are one of main shortcomings of the classical single-temporal data based maps.

As it was confirmed that the TS-FNF has higher reliability than the National forest map products used in Brazil and Peru, these maps will no longer be used in the JJ-FAST, but instead only the new ScanSAR TS-FNF will be used in for entire Latin America in a more consistent fashion. It should be noted that this is the first update of the forest mask since introducing FNF 2017 edition in May 2018. Due to the far superior reliability of the new map, a significant reduction in error detections related to incorrect land cover information (e.g., crop land and pasture) is expected.

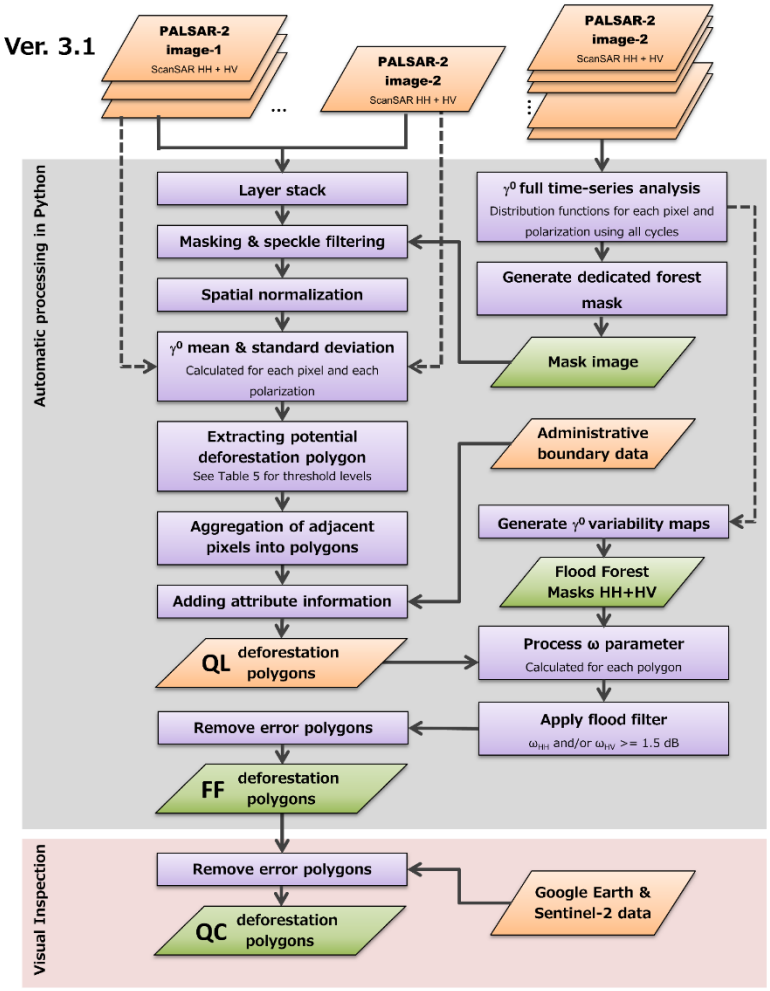

Fig. 9 Processing flow of deforestation detection algorithm Ver. 3.1.

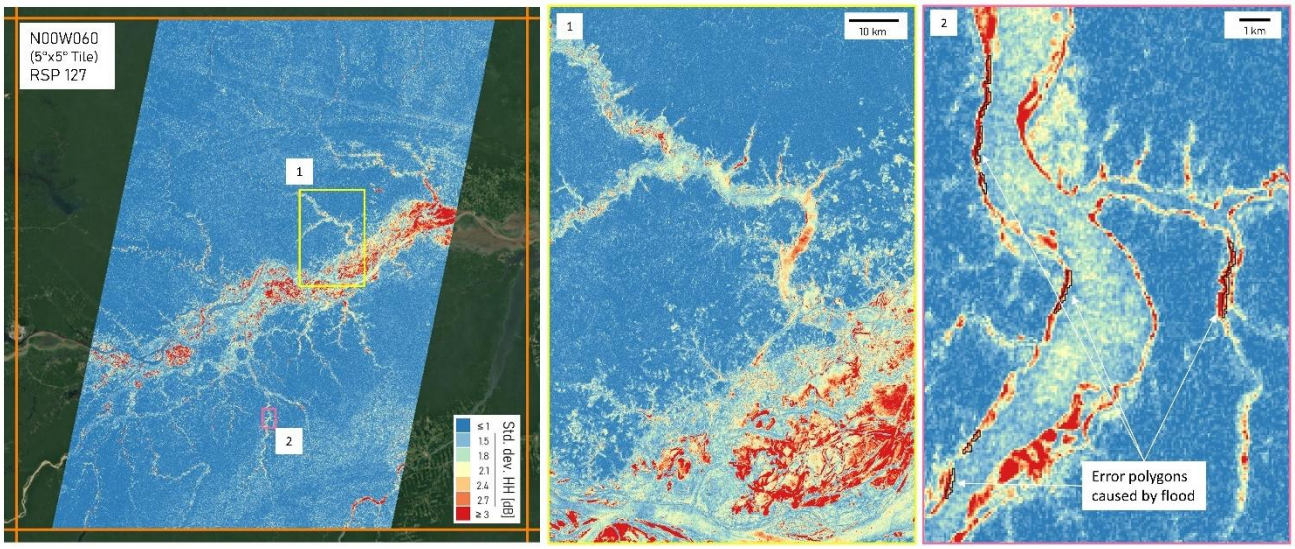

Fig. 10 New high-resolution flood forest mask based on ALOS-2/PALSAR-2 ScanSAR full time-series.

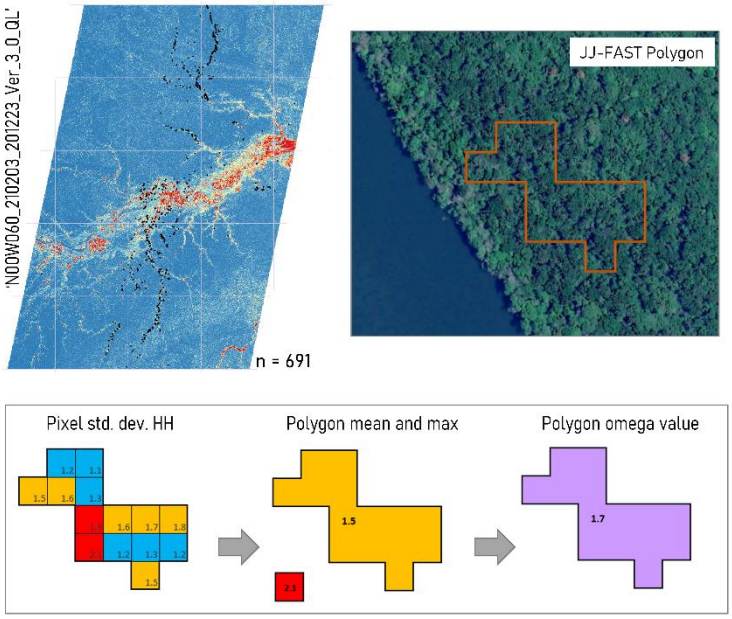

Fig. 11 Flood forest mask based false alarm suppression by omega parameter.

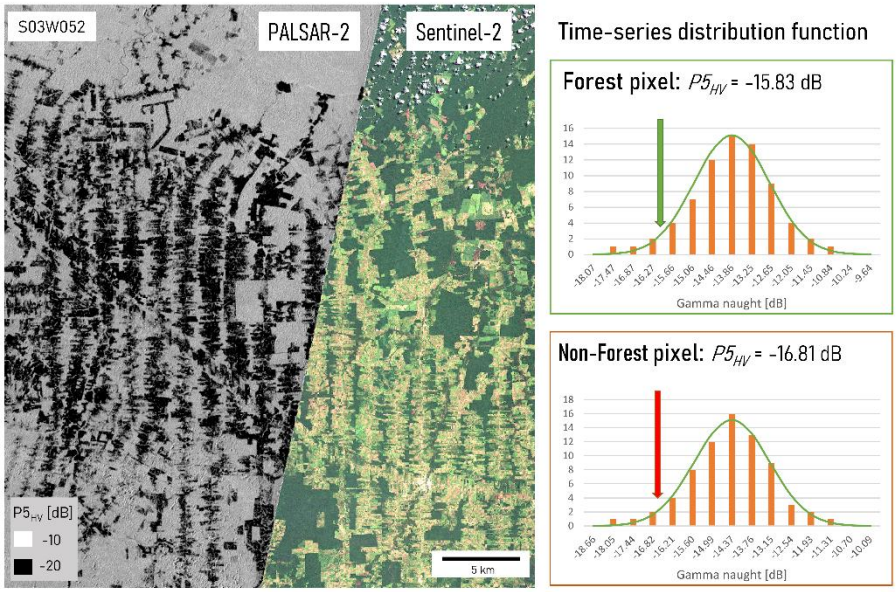

Fig. 12 Principle for full time-series based forest/non-forest classification.

Algorithm ver. 3.2 is the same processing procedure as Algorithm ver. 3.1. However, the basic processing software Sigma-SAR to generate the input PALSAR-2/ScanSAR image has been revised. This revision has improved the geolocation accuracy of PALSAR-2 image, and almost eliminated the shift between PALSAR-2 images at two different times, which was sometimes seen previously. As a result, error detections due to the shift has been substantially reduced. In addition, Ver. 3.2 is applied to the entire JJ-FAST target area, whereas Ver. 3.1 was applied only to Central and South America.

The Ver. 3.2 algorithm expands the use of the improved processing scheme, which Ver 3.1 previously introduced in Latin America only, to the entire JJ-FAST area. The advanced false alarm suppression and the new TS-FNF significantly

improve the user's accuracy in both Africa and Southeast Asia. Moreover, the basic ScanSAR processing software Sigma-SAR was upgraded from v2.4.0 to v3.0.0. The new processor version greatly improves the geolocation accuracy of PALSAR-2 ScanSAR images. As a result, error detections caused by unstable image geometry (i.e., shifted image pixels) have been largely eliminated.

5. Verification

To assess the early warning accuracy of the new Ver. 4.1 algorithm in the most reliable fashion possible, we employed a very strict validation procedure. At three test sites in the Brazilian legal Amazon, Planet daily imagery was used to map the forest loss conditions for 6 ALOS-2 observation cycles between 2020 and 2022. All deforestations occurring between 2 consecutive PALSAR observations during these periods were carefully mapped to allow a coherent validation of both user's and producer's accuracies. The number of cycles is limited, because these were the only terms where almost completely cloud free conditions allowed to create such a validation dataset from optical satellite data. Each of the test sites covers an area of 1° by 1° or approximately 110 km by 110 km. The test sites are located in the area of Porto Velho (s08W063) and Humaitá (S07W062) in the State of Rondonia as well as in Altamira (S02W052) in the state of Para (Fig. 11). Of course, the visual interpretation of optical images can realistically not be 100% correct. Especially phenological changes in the canopy are often very difficult to distinguish from actual deforestation. Therefore, a certain degree of uncertainty must be taken into account. However, we believe that the datasets are indeed reliable enough to obtain meaningful accuracy numbers. Moreover, most errors contained in the validation data sets will result in lower accuracy numbers for the ALOS-2 early warning performance. Hence the true accuracy of the new Ver. 4.1 should be rather underestimated than overestimated. An overview 'ground truth' data available for validation is shown in Table 2.

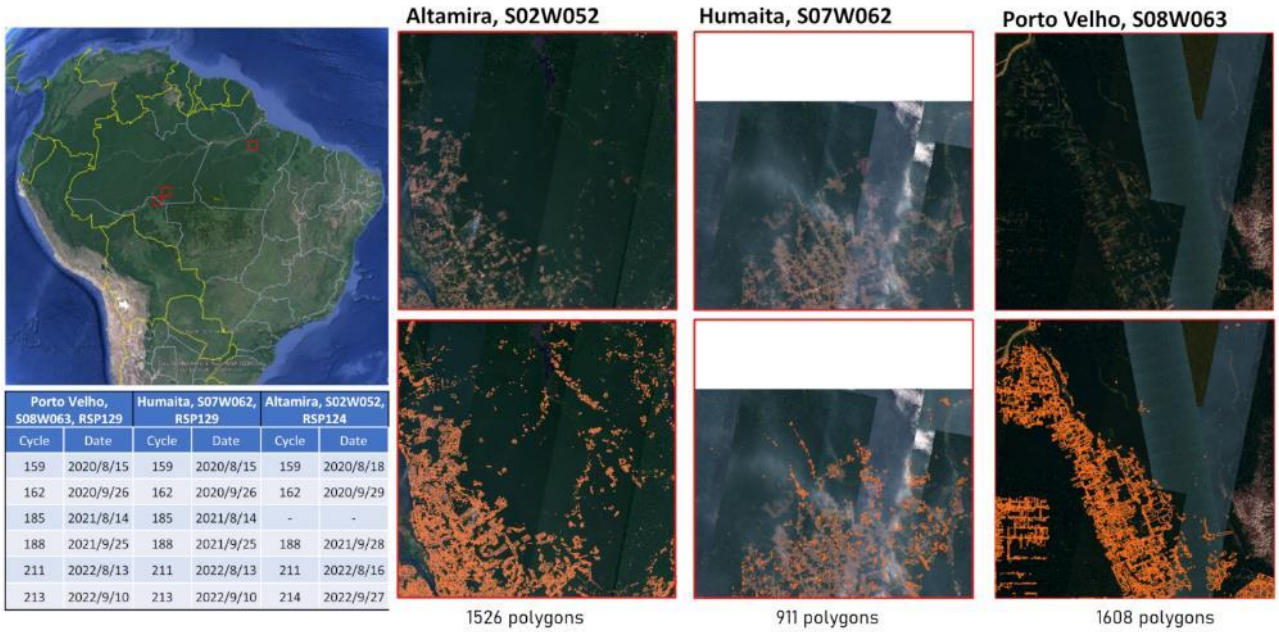

Porto Velho, S08W063, RSP129		Humaita, S07W062, RSP129		Altamira, S02W052, RSP124	
Cycle	Date	Cycle	Date	Cycle	Date
159	2020/8/15	159	2020/8/15	159	2020/8/18
162	2020/9/26	162	2020/9/26	162	2020/9/29
185	2021/8/14	185	2021/8/14	-	-
188	2021/9/25	188	2021/9/25	188	2021/9/28
211	2022/8/13	211	2022/8/13	211	2022/8/16
213	2022/9/10	213	2022/9/10	214	2022/9/27

Fig. 13 Three validation and calibration super sites in the Brazilain Legal Amazon.

Table 5 Overview of Planet based 'ground truth' data for three large-scale validation sites in Brazil.

Test site		Altamira	Humaitá	Porto Velho
Location		S02W052	S07W062	S08W063
Area (km^2)		12298	12206	12177
RSP path		123, 124	128, 129	129, 130
Cycle	Season	Ground truth polygon count		
159	Aug/2020	119	108	315
162	Sep/2020	304	213	260
185	Aug/2021	176	165	308
188	Sep/2021	329	173	364
208	Aug/2022	230	138	203
211	Sep/2022	368	114	158
	Sum	1526	911	1608

From the available validation efforts, using some 4045 deforestation cases distributed over the three 1° by 1° validation sites and 6 different dates, it was confirmed that the producer's accuracy range between 38.2% and 62.4% depending mainly on seasonal and rainfall conditions. The user's accuracy ranged between 49.3% and 75.7%. The average producer's accuracy and user's accuracy taking into account all validation data combined is 44.5% and 64.2%, respectively. It is important to note that in this study we consider a true detection exclusively as the case where the forest cover loss occurred before the last observation and after the previous observation, i.e., between the 2 latest image acquisitions. Given the nominal repeat interval of 42 -days (every third repeat cycle) plus the 3-days required for processing the PALSAR-2 data to obtain the final deforestation polygons and publish them online, this implies that a fresh and ongoing logging activities can be not older than 45-days in the worst case. In many hot spot areas in the amazon basin the repeat intervals are only 28 days (every second repeat cycle), and in some rarer cases even up to 14 days (1 repeat cycle). Moreover, for the trained eye it is easy to tell which of the polygons are "live" and have priority to be inspected by authorities. The average time lag between start of deforestation activities and successful detection by ALOS-2 was 15 days. This should be well enough time to act on most of the early warning produced by the Ver. 4.1 algorithm.

To test the potential to adjust the Ver. 4.1 algorithm to specific users' requirements three different parameter models were developed with A) optimized for highest user's accuracy, C) optimized for highest producer's accuracy, and B) and intermediate model optimized for a balance between user's and producer's accuracy. The detailed validation results for each cycle and each test site are shown in Fig. 12. The summary and final overall accuracy numbers for the 3 parameter A, B, and C are shown in Fig. 13. The comparison with Ver. 4.0 and Ver. 3.2 demonstrates the improved performance of the latest JJ-FAST algorithm.

Note that based on the user requirements in the Amazon area, parameter setting A is used in South America, whereas parameter setting B is adopted in all other JJ-FAST regions, i.e. Central America, Africa, and South and

Southeast Asia.

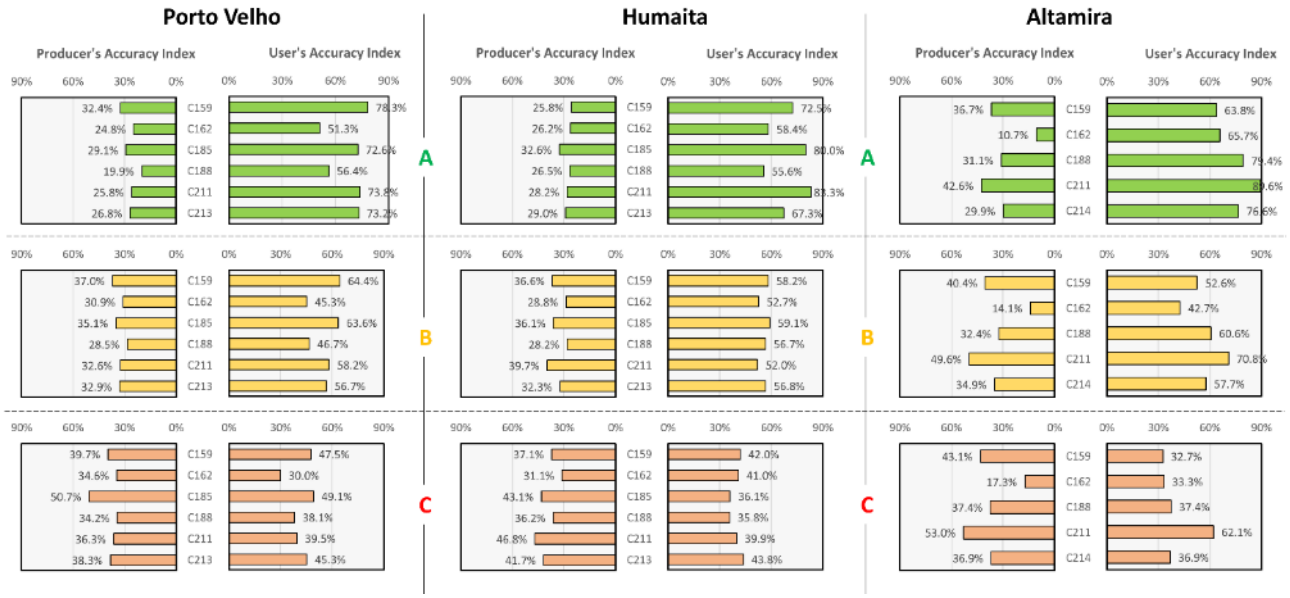

Fig. 14 Detailed validation results for the three parameter settings A, B, and C for each test site and each observation cycle.

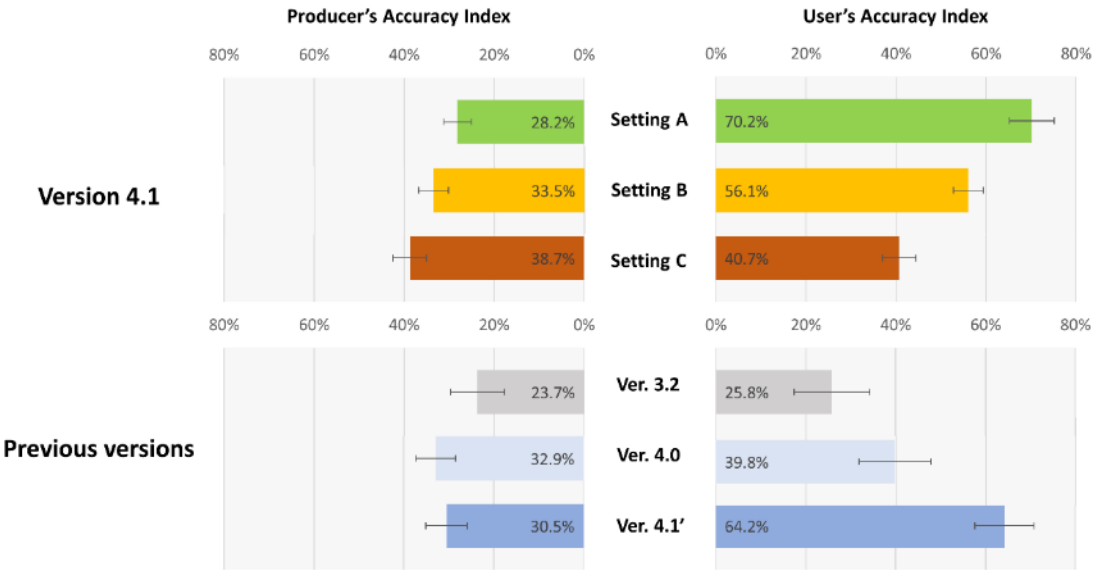

Fig. 15 Overall accuracy of the three parameter settings A, B, and C of Ver 4.1 and comparison with previous algorithm generations Ver. 4.0 and Ver. 3.2.

Figure 14 shows some validation examples of JJ-FAST early warning polygons. The examples taken from a recent observation in the Altamira test site during ALOS-2 observation cycle 240 on 26 September 2023 demonstrate the

unique capability of the PALSAR-2 data and the next-generation early warning algorithm to detect fresh and ongoing deforestation in the humid tropical forest areas.

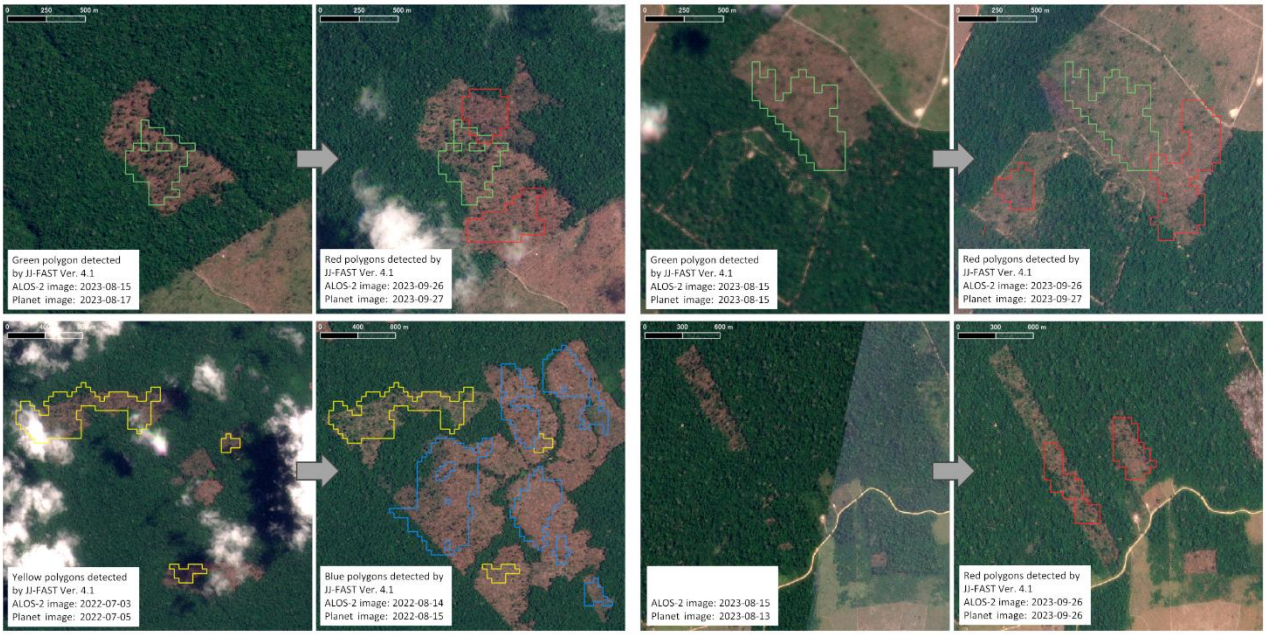

Fig. 16 Examples of early warning polygons detected by the fully automatic JJ-FAST Ver. 4.1 algorithm in the Altamira Cal/Val site, State of Para, Brazil. (Images © Planet Labs).

6. Two types of Old JJ-FAST products, QL and QC (discontinued)

From 1 July, 2019, to 17 April 2023, JJ-FAST has been delivering two types of polygon products for JJ-FAST Ver 2.x and Ver. 3.x, namely Quick Look (QL) and Quality Checked (QC). QL products were available shortly after the ALOS-2 observations with a delay of only 3-4 days. Polygons distributed via the QL products contain all deforestations detected by the Old JJ-FAST algorithm. Note that the QL deforestation polygons are validated and therefore show significantly higher false alarm rates and low accuracy. The usual “Quality Checked” (QC) products with validated deforestation polygons will be released 4-7 days after the observations as always. The locations of the latest QL and QC detections are shown as purple and red pins on the JJ-FAST map, respectively. As before, the locations of all past deforestation detections will be shown as yellow pins.

For archived JJ-FAST data from the given period, users can select the QC or QL polygons by using the Data Select menu in which QL polygons can be identified by text “(QL)” in the list (Fig.11) and QC polygons are listed in observation term only (without (QL)).

The filename of QL products has a string “_QL” before extension (e.g. S10W062_190701_190422_02_QL.shp).

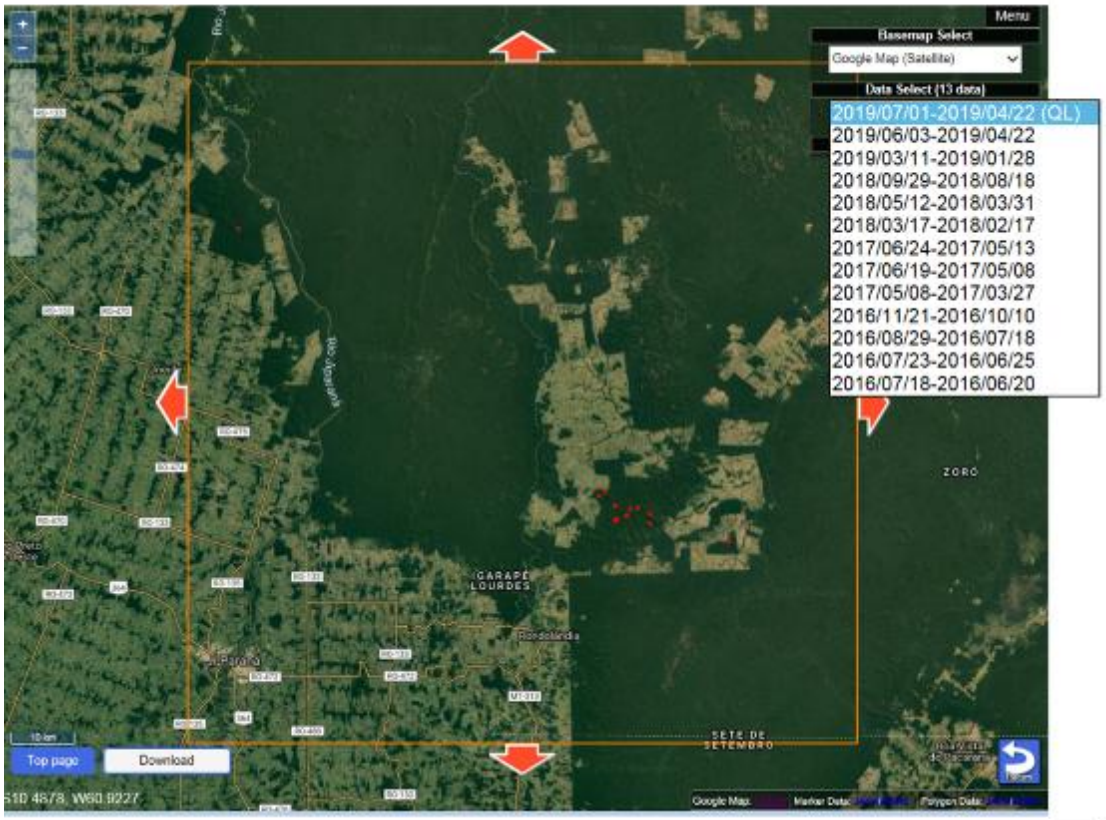

Fig. 17 Example of the Data Selection.

7. Bibliography

■ **Academic journals**

Shimada, M. et al. (2014): New global forest/non-forest maps from ALOS PALSAR data (2007–2010), *Remote Sensing of Environment*, 155, 13-31. https://doi.org/10.1016/j.rse.2014.04.014

Motohka, T. & Hayashi, M. (2017): Forest observation from space by the satellite Daichi-2. *Seibutsu-no-kagaku Iden*, 71(1), 70-76. [in Japanese]

Watanabe, M. et al. (2018): Early-stage deforestation detection in the tropics with L-band SAR, *IEEE Journal of Selected Topics in Applied Earth Observations and Remote Sensing*, 11(6), 1-7. https://doi.org/10.1109/JSTARS.2018.2810857

Koyama, C. et al. (2019): Mapping the spatial-temporal variability of tropical forests by ALOS-2 L-band SAR big data analysis, *Remote Sensing of Environment*, 233, 111372.

Watanabe, M. et al. (2021): Refined algorithm for forest early warning system with ALOS-2/PALSAR-2 ScanSAR data in tropical forest regions, *Remote Sensing of Environment*, 265, 112643.

■ **Book**

Shimada, M. (2018): Imaging from spaceborne and airborne SARs, Calibration, and Applications, CRC press.

■ **Conference proceedings**

Watanabe, M. et al. (2016): Examination of a method of early deforestation detection (advanced) using PALSAR-2/ScanSAR for JICA-JAXA Forest Early Warning System in the Tropics (JJ-FAST). *Journal of the Remote Sensing Society of Japan,* 61, p. 21.

Ogawa, T. et al. (2016): Examination of a method of extracting changes and the results of a prototype production in JICA-JAXA Forest Early Warning System in the Tropics (JJ-FAST). *Journal of the Remote Sensing Society of Japan,* 61, p. 257.

Koyama, C.N. et al. (2016): Fundamental study on soil moisture variations under vegetation influencing L-band SAR backscatter – implementations for the development of an advanced forest monitoring system. Proc. of 61th Autumn Conference of the Remote Sensing Society of Japan, Nov. 1-2, Niigata, Japan, pp. 145-146.

Hayashi, M. et al. (2017): Deforestation detection using ALOS-2/PALSAR-2 for JICA-JAXA Forest Early Warning System in the Tropics (JJ-FAST). *Journal of the Japanese Forest Society*, 128 https://www.jstage.jst.go.jp/article/jfsc/128/0/128_44/_article/-char/ja/ (Access in September, 2017)

Hayashi, M. et al. (2017): ALOS-2/PALSAR-2 utilization for deforestation detection in JICA-JAXA Forest Early Warning System in the Tropics (JJ-FAST). International Symposium on Remote Sensing 2017.

Watanabe, M. et al. (2017): Early-stage deforestation areas observed with L-band (PALSAR-2) and C-band (Sentinel-1) SAR. International Symposium on Remote Sensing 2017.

Watanabe, M. et al. (2017): Examination the 3rd of early deforestation detection method (advanced) using PALSAR-2/ScanSAR for JICA-JAXA Forest Early Warning System in the Tropics (JJ-FAST). – Results of time-sequential analysis in South America –. JpGU-AGU Joint Meeting 2017.

Hayashi, M. et al. (2017): Deforestation detection using ALOS-2/PALSAR-2 imagery in JICA-JAXA Forest Early Warning System in the Tropics (JJ-FAST). 31st International Symposium on Space Technology and Science (ISTS).

Watanabe, M. et al. (2017): Development of early-stage deforestation detection algorithm (advanced) with palsar-2/scansar for jica-jaxa program (jj-fast). IEEE International Geoscience and Remote Sensing Symposium (IGARSS) 2017.

Watanabe, M. et al. (2017): Polarimetric characteristics of L-band SAR images of early-stage deforestation areas. IEEE International Geoscience and Remote Sensing Symposium (IGARSS) 2017.

Koyama, C.N. et al. (2017): The Effect of Precipitation and Soil Moisture Variations on (Partial) Polarimetric L-band SAR Backscatter in Tropical Forest regions. Proc. of IEEE International Geoscience and Remote Sensing Symposium (IGARSS), July 23-28, Fort Worth, USA, pp. 2719–2722.

Koyama, C.N. et al. (2018): Tropical forest classification based on multi-temporal ALOS-2/PALSAR-2 ScanSAR observations. Proc. of 65th Autumn Conference of the Remote Sensing Society of Japan, pp. 51-52.

Watanabe, M. et al. (2019): Improvement of Deforestation Detection Algorithms used in JJ-FAST, IEEE International Geoscience and Remote Sensing Symposium (IGARSS) 2019, July 28 – August 2, Yokohama, Japan, pp. 5328–5331.

Koyama, C.N. et al. (2019): Mapping Spatial-Temporal Forest Heterogeneity in the Tropical Belt by ALOS-2/PALSAR-2 Big Data Analysis, IEEE International Geoscience and Remote Sensing Symposium (IGARSS) 2019, July 28 – August 2, Yokohama, Japan, pp. 5336–5339.

Nagatani, I. et al. (2019): Pixel-Based Deforestation Detection Algorithm for ALOS-2/PALSAR-2, IEEE International Geoscience and Remote Sensing Symposium (IGARSS) 2019, July 28 – August 2, Yokohama, Japan, pp. 5332–5335.

Nagatani, I. et al. (2020): Seasonal Change Analysis for ALOS-2 PALSAR-2 Deforestation Detection, IEEE International Geoscience and Remote Sensing Symposium (IGARSS) 2020, September 26 – October 2, Virtual Event, pp. 3807–3810.

Watanabe, M. et al. (2020): Trial of Deforestation Detection by Using 25m Resolution PALSAR-2/ScanSAR Data, IEEE International Geoscience and Remote Sensing Symposium (IGARSS) 2020, September 26 – October 2, Virtual Event, pp. 3784–3787.

Koyama, C.N. et al. (2020): Rainfall-Induced Changes in L-Band Backscatter Over Tropical Forests and Their Impact on Deforestation Monitoring, IEEE International Geoscience and Remote Sensing Symposium (IGARSS) 2020, September 26 – October 2, Virtual Event, pp. 3799–3802.

Koyama, C.N. et al. (2021): Improving L-Band SAR Forest Monitoring by Big Data Deep Learning Based on ALOS-2 5 Years Pan-Tropical Observations, IEEE International Geoscience and Remote Sensing Symposium (IGARSS) 2019, July 12 – 16, Virtual Event, pp. 6747–6500.

Watanabe, M. et al. (2021): Trial of Detection Accuracy Improvement for JJ-FAST Deforestation Detection Algorithm Using Deep Learning, IEEE International Geoscience and Remote Sensing Symposium (IGARSS) 2019, July 12 – 16, Virtual Event, pp. 2911–2914.

Koyama, C.N. et al. (2021): Assessing the Impact of Precipitation on L-band SAR Forest Observation: An ALOS-2 Big Data Case Study in the Tropics, 13th European Conference on Synthetic Aperture Radar (EUSAR 2021), March 28 – April 1, Virtual Event, 2021, pp. 1-6.

Koyama, C.N. et al. (2021): Long-Term Pantropical Forest Monitoring with ALOS-2 L-Band SAR, 7th Asia-Pacific Conference on Synthetic Aperture Radar (APSAR 2021), November 1 – 3, Virtual Event, pp. 1-5.

Koyama, C.N. et al. (2022): ALOS-2 – The Pioneer Mission for L-band SAR Long-term Pantropical Forest Monitoring, 33rd International Symposium on Space Technology (ISTS 2022), February 28 – March 4, Virtual Event, pp. 1-6.

Koyama, CN et al. (2022): Advancements in global forest monitoring research founded on ALOS-2 long-term pantropical land observation, IGARSS 2022, Online, July 17-22, pp. 4445-4448.

Koyama, CN et al. (2022): ALOS-2/PALSAR-2 Long-term Pantropical Observation – A Paradigm Shift in Global Forest Monitoring, EUSAR 2022, Leipzig, Germany, July 25-27, pp. 116-120.

Koyama, CN et al. (2022): Extending JAXA's long-term L-band SAR forest observation legacy with ALOS-4/PALSAR-3, SPIE Sensors & Imaging, Berlin, Germany, Sept 5-8, 1226408.

Koyama, CN et al. (2022): Next-generation L-band SAR deforestation algorithm for highly-accurate operational early warning in tropical forests, Proc. of 73rd Autumn Conference of the Remote Sensing Society of Japan, Nov 29-30, pp. 1-4.

Koyama, CN, et al. (2023): ALOS-2's Contributions to Sustainable Development Goals – Making Operational Early Warning and Near Real-Time Forest Loss Assessment a Reality Today, 34th International Symposium on Space Technology (ISTS 2023), June 3-9, Kurume, Japan, pp. 1-5.

Koyama, CN, et al. (2023): Next-generation L-band SAR deforestation detection for operational forest early warning in the tropics, IGARSS 2023, July 16-21, Pasadena, USA, pp. 2633–2636.

Koyama, CN, et al. (2023): Achievements of the ALOS-2 L-band SAR long-term pantropical forest monitoring mission, IGARSS 2023, July 16-21, Pasadena, USA, pp. 1994–1997.

Koyama, CN, et al. (2023): From ALOS-2 to ALOS-4: Japan's pioneering L-band SARs for global vegetation monitoring - state-of-the-art and future perspectives, SPIE Sensors & Imaging 2023, Sep 3-6, Amsterdam, The Netherlands, 1226408.

Koyama, CN et al. (2024): Deforestation Detection and Early Warning using L-band SAR, EUSAR 2024, Munich, Germany, April 23-26, pp. 116-120.

Koyama, CN et al. (2025): ALOS-2/-4 Operational Deforestation Detection and Early Warning – Japan's L-band SAR Contribution to Global Forest Sustainability, 9th Asia-Pacific Conference on Synthetic Aperture Radar (APSAR 2021), October 5– 9, Matsue, Japan, pp. 1-5.

Koyama, CN et al. (2025): ALOS-2 Long-Term Observation of the Legal Amazon - Monitoring Deforestation, Forest

Loss, and Regrowth by L-band SAR, 2025 IEEE Latin American GRSS + ISPRS Remote Sensing Conference (LAGIRS 2025), November 10–13, Foz do Iugacu, Brazil, pp. 42-46.

8. Staff

■ JICA Global Environment Department	Mr. Genya Nakamura
	Mr. Masaru Kurimoto
	Ms. Sayako Kishimoto
■ JAXA Earth Observation Research Center	Dr. Takeo Tadono
	Dr. Christian Koyama
	Ms. Yukari Yamazaki
■ Remote Sensing Technology Center	Mr. Tomohiko Higashiuwatoko
	Dr. Osamu Isoguchi
	Mr. Kazufumi Kobayashi
	Mr. Takafusa Andoh

■ Former Staff

■ JICA Global Environment Department	Mr. Kenichi Shishido
	Mr. Takahiro Morita
	Ms. Kanako Adachi
	Mr. Ichiro Mimura
	Ms. Yoko Makita
	Ms. Mari Miura
	Dr. Hiroaki Okonogi
	Mr. Takashi Nishimura
	Mr. Takahiro Ikenoue
	Mr. Hideo Noda
■ JAXA Earth Observation Research Center	Mr. Yutaka Kaneko
	Dr. Izumi Nagatani
	Mr. Tomohiro Watanabe
	Dr. Masato Hayashi
	Ms. Erina Sakaguchi
	Ms. Yumiko Fujita
■ Tokyo Denki University	Prof. Masanobu Shimada
	Dr. Manabu Watanabe
■ Remote Sensing Technology Center	Dr. Tsutomu Yamanokuchi
	Mr. Takeshi Ogawa

9. Contact point

Please contact us from the question form of the following URL.

Contact Us (https://www.eorc.jaxa.jp/jjfast/jj_inquiery.html)

Appendix

A1. Previous algorithm generations

■ Algorithm Ver. 0.0

Algorithm Ver. 0.0 was used from the start of operation in November 2016 to June 2017 (Fig. A1). This algorithm is processed by a program described in ArcPy script that basically runs on ESRI's ArcGIS.

The main input data are two HV cross-polarized PALSAR-2 ScanSAR images acquired on different dates (one before and one after deforestation). These images are processed to analysis ready data by the SigmaSAR PALSAR-2 processor and subsequently divided into 1°×1° tiles. The before and after images are combined to one data set and areas all pixels not suitable for further processing, such as non-forest areas, steep slopes, and overlays, are masked out. Here, the ALOS/PALSAR based forest and non-forest maps (Shimada et al., 2014) are used for masking out non-forest areas. Note that some uncertainties can occur due to the definition of forest in the map does not completely match with individual the forest definitions in each target country. Because the radar shadow and overlay that are peculiar to the images of synthetic aperture radars such as PALSAR-2, occur, such phenomena are excluded using the mask images of steep slope areas and the correction area images output from the basic processing software SigmaSAR.

Next, segmentation (mean-shift method) is performed to divide the image into small polygons that are similar in characteristics. Then, all polygons where the averaged backscatter coefficient γ^0 shows a substantial decrease are extracted as a candidate for deforestation sites. Specifically, we extract two types of polygons: one varies by -5 dB or more and the other varies by -3 to -5 dB. Each of these candidate polygons of deforestation has position information, etc., added as attribute information. In addition, polygons with an area smaller than 5 ha are removed because a lot of false detections can occur due to the effects of radar speckle and other image noise. The bright polygons of the first image with -5 dB or more are also eliminated because of the vague influential range of overlay or a high possibility of non-forest areas like an urban area.

The polygons created by automatic processing are characterized by high false alarm rates. In order to make them final deliverables, we refer to high-resolution optical satellite images of Google Earth and LANDSAT time-series images to verify the detected deforestation polygons by visual interpretation before they are published online.

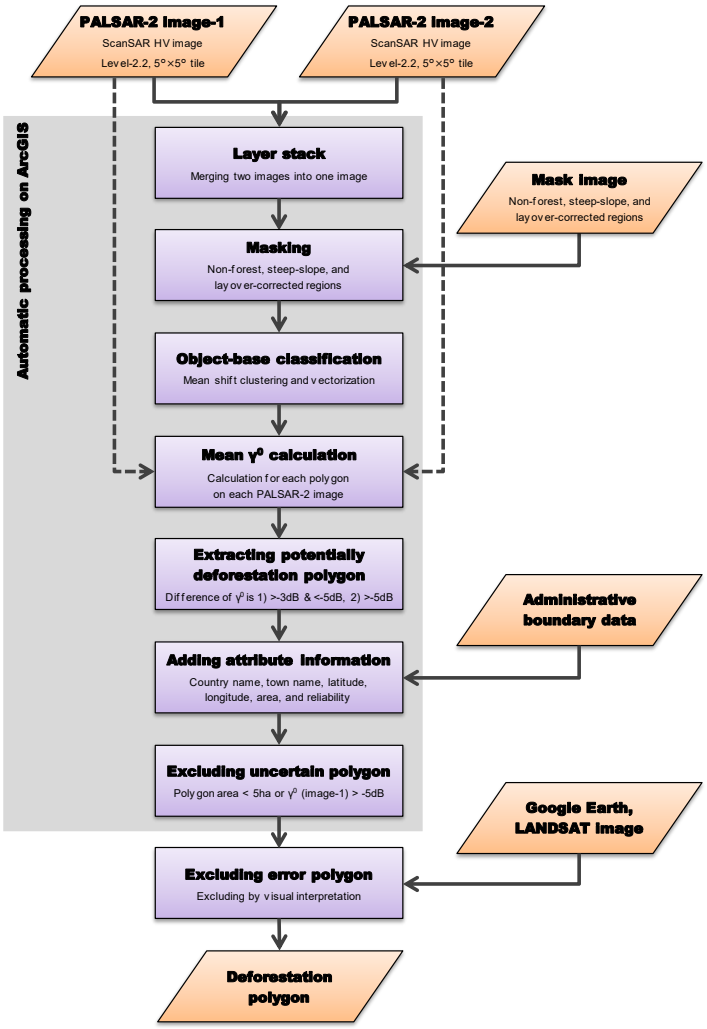

Fig. A1 Processing flow of deforestation detection algorithm Ver. 0.0

■ Algorithm Ver. 1.0

Algorithm Ver. 1.0 has been used from July 2017 to April 2018 (Fig. A2). In this algorithm, the program described in the ArcPy script in Ver. 0.0 is transferred into a stand-alone Python computer program. Using only Python libraries, the ArcGIS routines are no longer required. The main difference from the Ver. 0.0 algorithm is associated with the object classification, in which it is not vectorized immediately after the segmentation by the object classification but is integrated with similar segments by a classification process.

Furthermore, we updated the forest map data (for non-forest region mask) to reduce false detections in misclassified non-forest areas. Notably, the 2010 version of PALSAR forest and non-forest map was replaced with the 2016 version of PALSAR-2 map. In addition, some governmental forest maps were adopted regionally.

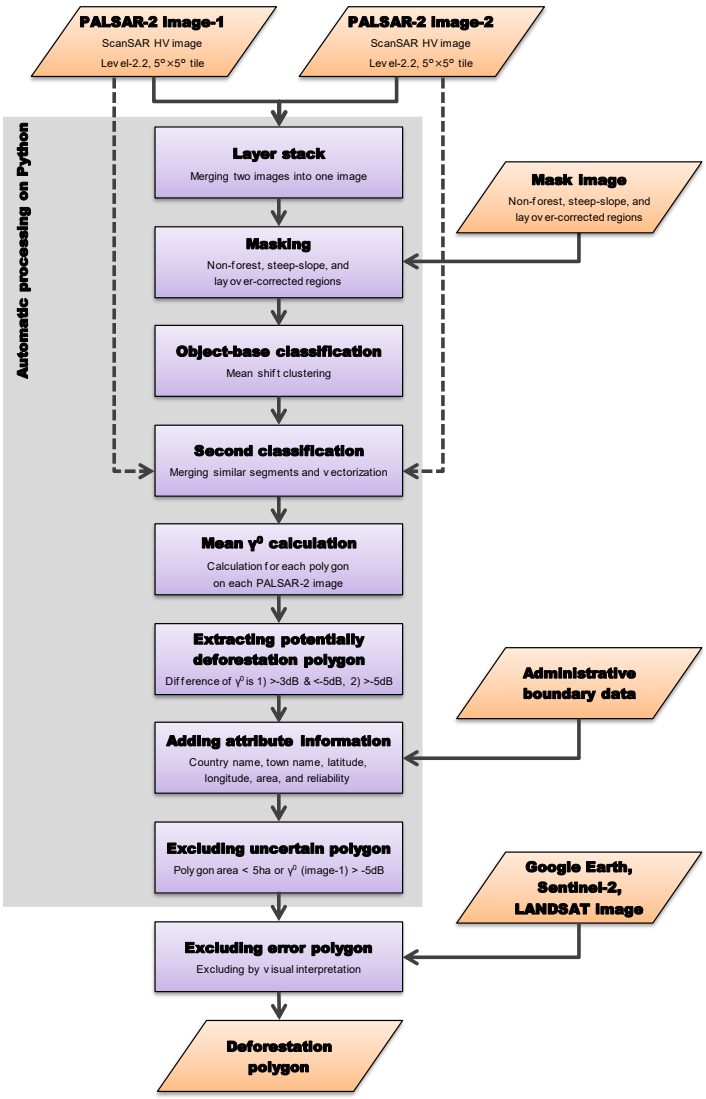

Fig. A2 Processing flow of deforestation detection algorithm Ver. 1.0

■ Algorithm Ver. 2.0

Algorithm Ver. 2.0 has been used from April 2018 to June 2019 (Fig. A3). The main input data are PALSAR-2 time-series images, employing the HV and HH polarization images observed in ScanSAR mode. These images are corrected for geometric and topographic effects (ortho-rectification and slope correction) using the Sigma-SAR processor for PALSAR-2 and subsequently divided into 1°×1° tiles. These data are stacked into a 3-dimensional dataset and a mask image is created from non-forest areas, urban areas, steep slope, and overlays images. The ALOS-2/PALSAR-2 forest and non-forest maps (Shimada et al., 2014) were combined with some government-approved forest maps in some countries (Peru, Botswana, and Brazil), to increase the reliability. Radar shadow and overlay areas that are characteristic features in synthetic aperture radar imaging are excluded by mask processing.

Next, segmentation-based object classification (K-means method) is performed to divide the image into small polygons that are similar in characteristics. Then, we will extract a polygon where the average of backscatter coefficient γ^0 meets some criteria (Table A1). The PALSAR-2 observes the signals that are scattered backward from the ground surface by emitting microwaves from its onboard antenna. The HV polarization image changes from bright to dark in a deforestation area, because forest areas looks bright due to many backscattered components and a non-forest area looks dark due to specular reflection of most of the microwaves (Fig. A4). The HV polarization algorithm applied to global area. The HH polarization image and HH/HV ratio image are used for detecting various deforestation conditions (Watanabe, et al., 2018). The HH polarization image can detect deforestation sites, where freshly felled trees are left on the ground. The HH/HV ratio can detect deforestation sites, where felled trees left on the ground have already been burned. The HH and HH/HV ratio algorithm are applied to South East Asia and America. We use the PALSAR-2 time-series images to improve the accuracy. In Fig. 4, the "PALSAR-2 image-2" means target image for deforestation detection, which is the latest observed image in the analysis. On the other hand, "PALSAR-2 image-1" means reference images, which are at most 10 images in April 23- July 15, 2018 and 15 images in July 16, 2018 – June 29, 2019. We compare the average value of γ^0 for each polygon between "PALSAR-2 image-1" and "PALSAR-2 image-2" to detect deforestation. In addition, polygons with an area smaller than 3 ha are because a lot of false detections can occur due to the effects of radar speckle and other image noise.

The polygons created by automatic processing are characterized by high false alarm rates. In order to make them final deliverables, we refer to high-resolution optical satellite images of Google Earth and LANDSAT time-series images to verify the detected deforestation polygons by visual interpretation before they are published online.

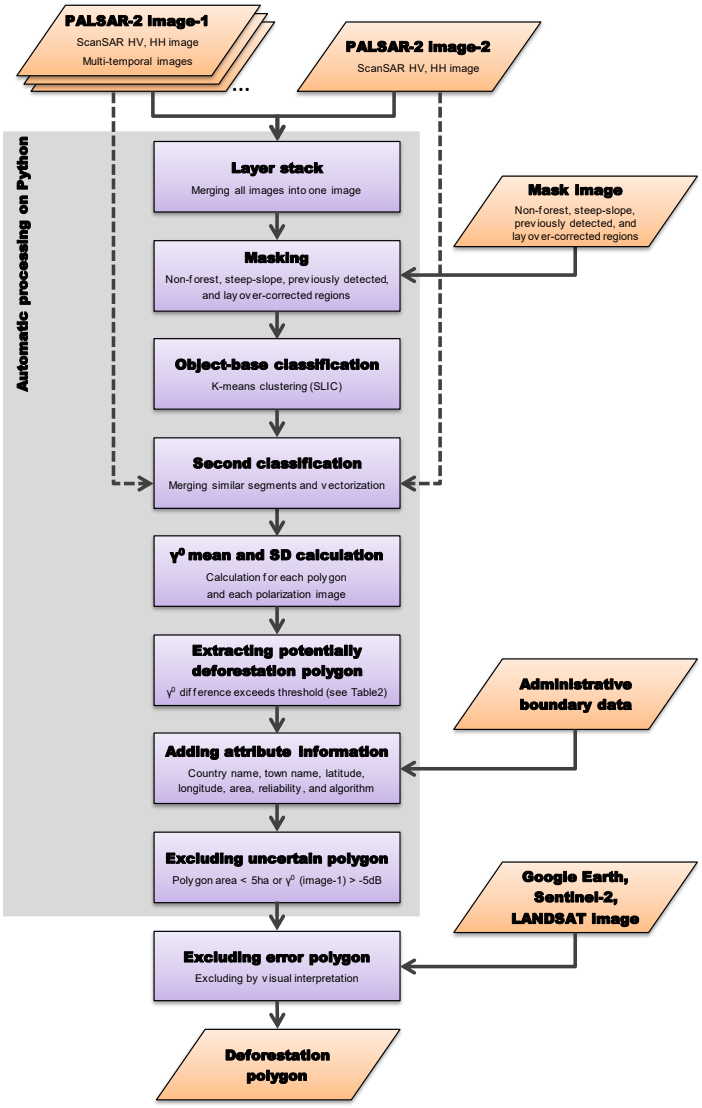

Fig. A3 Processing flow of deforestation detection algorithm Ver. 2.0

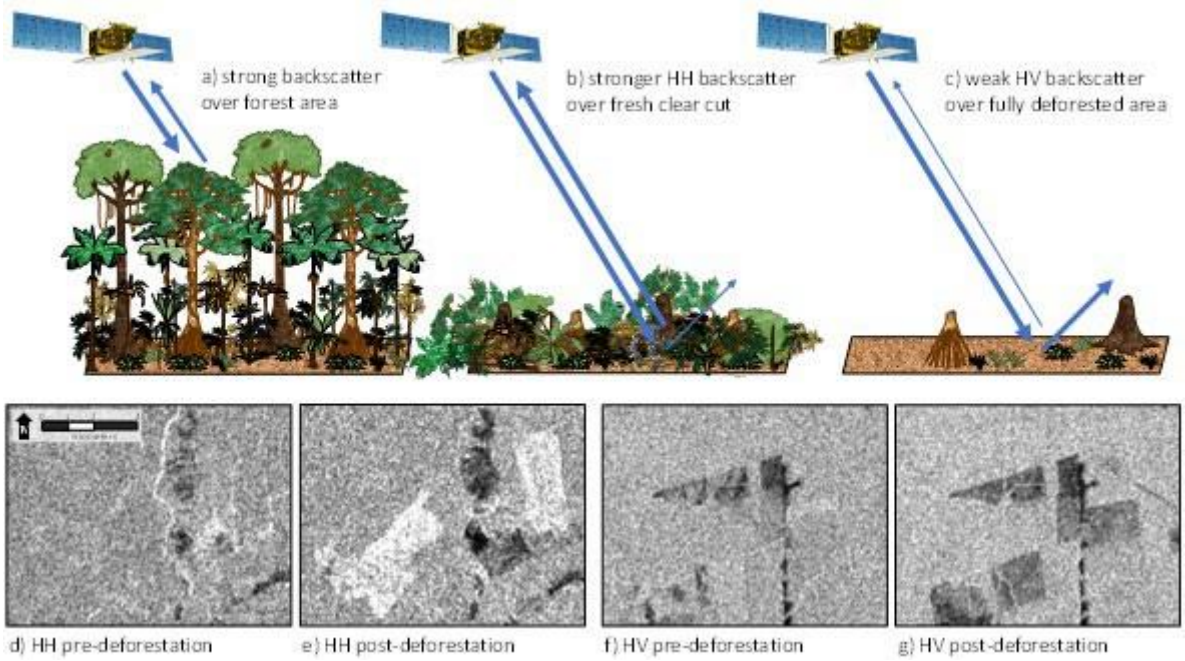

Fig. A4 Schematic of the deforestation detection principle by increasing HH backscatter (a, b, d, e) or decreasing HV backscatter (a, c, f, g).

Table A1 Threshold values for deforestation detection

Methodology	Level-1	Level-2
Using HV polarization images	-4.0 dB	-3.0 dB
Using HH polarization images	+3.0 dB	+ 2.0 dB
Using HH/HV ratio	+3.2	+ 2.0

■ Algorithm Ver. 2.1

Algorithm Ver. 2.1 has been used from July 2019 to May 2020 (Fig. A5). The Algorithm is principally same as Ver. 2.0 but the number of time series images was increased to 20 images (Table 4) and the threshold values were reviewed and optimized (Table A2).

Due to the large γ^0_{HH} seasonal variations, especially in the dry forest areas, the HH and HH/HV ratio algorithm are applied to only some selected areas shown in Fig. 7. The criteria for the selected area are that temporal standard deviation of γ^0_{HH} is less than 0.7 dB (Koyama et al., 2019) and forest biomass is more than 100 t/ha (based on LUCID, Land use, carbon & emission data, http://lucid.wur.nl/). Finally, we categorized two levels of polygons: level-1 of high reliability deforestation and level-2 of medium reliability deforestation.

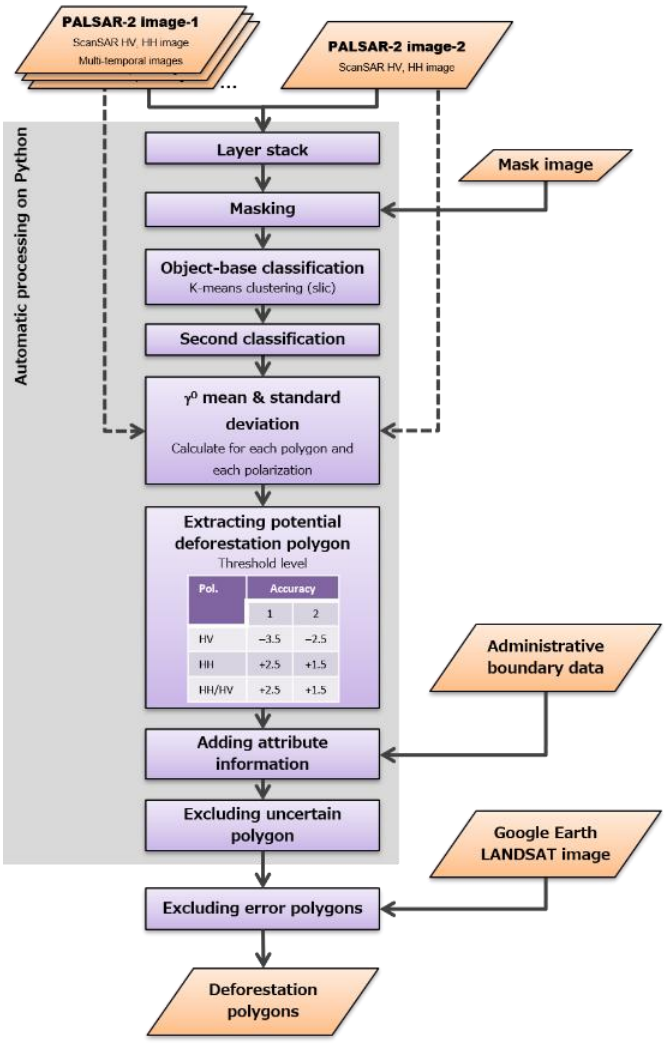

Fig. A5 Processing flow of deforestation detection algorithm Ver. 2.1.

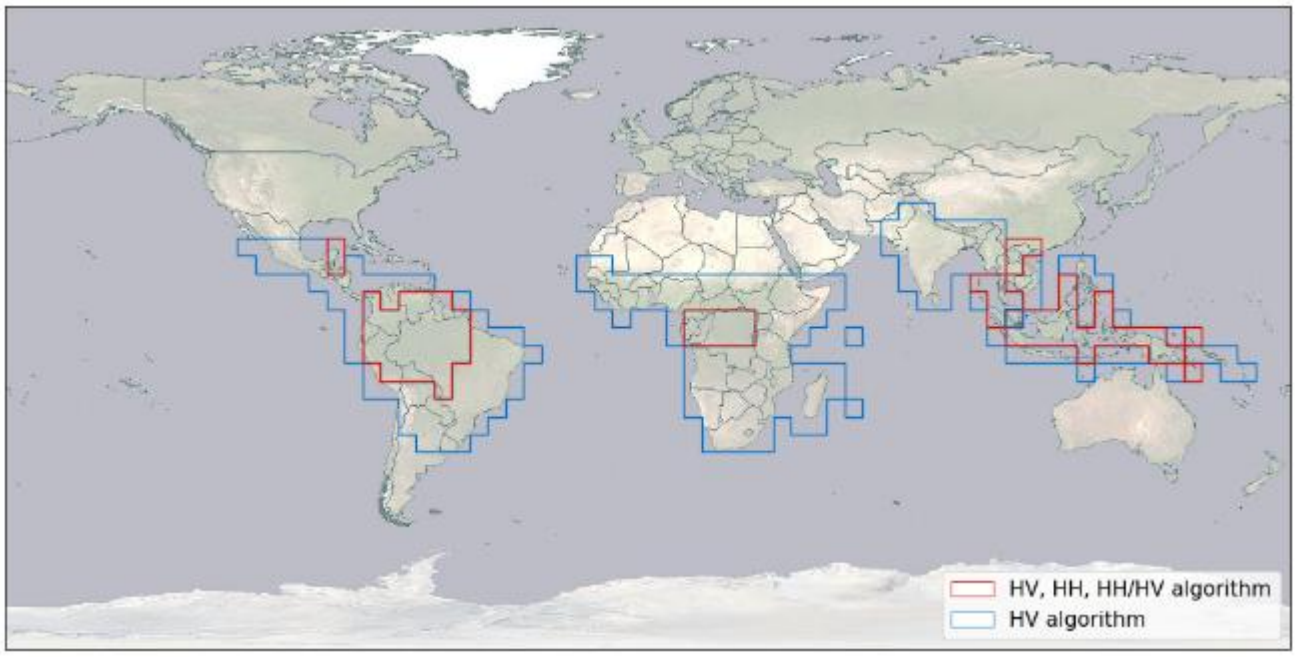

Fig. A6 The area definitions for the use of HV, HH and HH/HV ratio algorithm (red) and the HV-only algorithm

(blue).

Table A2 Threshold values for deforestation detection

Methodology	Level-1	Level-2
Using HV polarization images	-3.5 dB	-2.5dB
Using HH polarization images	+2.5 dB	+1.5 dB
Using HH/HV ratio	+2.5	+1.5

■ Algorithm Ver. 3.0

Algorithm ver. 3.0 has been used since June 2020 (Fig. A7). There are three major updates from ver. 2.1, and the minimum detection size are minimized from 3.0 ha to 2.0 ha.

1) Data process unit: polygon $\rightarrow$ pixel

2) Applying spatial normalization

3) Threshold level depending on the site.

Data process unit is changed from polygon to pixel so that the detection size is enabled to minimize from 3.0 to 2.0 ha. Lee-sigma speckle filter with window size of 5×5 pixel is applied to suppress the speckle.

Temporal normalization is a technique that an area taken by latest data is temporally normalized by the past data, and are applied to suppress the error detection, caused by regional γ^0 change induced by seasonal change, or flood occurred in a forest (see fig. 16-a).

Version 2.1 algorithm shows better detection accuracies for the sites, where the number of detections is relatively small. On the other hand, the sites where many deforestations happen, shows lower producer's accuracies. Then, smaller threshold levels are introduced for some sites to improve the producer's accuracies. The sites, where many deforestations happen, were selected, and apply the algorithm with smaller threshold value. The site, where the producer's accuracies were improved, were picked up. The sites introduced the smaller threshold level, are plotted in Fig. A8, and the threshold values are summarized in Table A3.

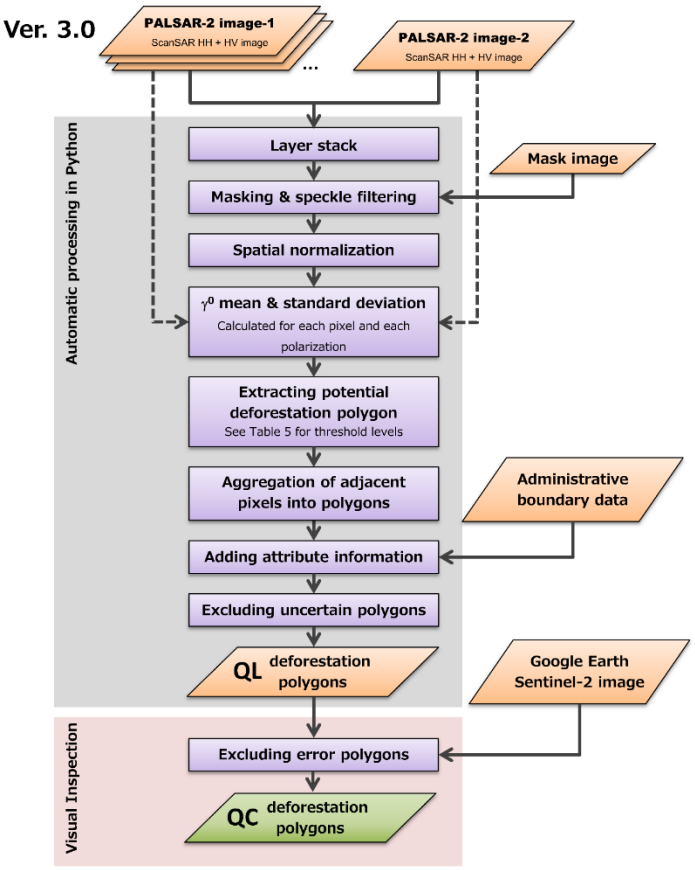

Fig. A7 Processing flow of deforestation detection algorithm Ver. 3.0.

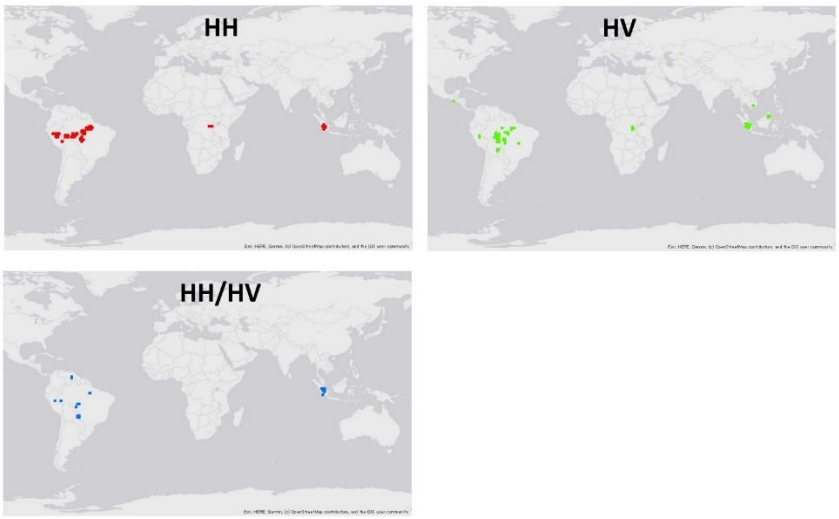

Fig. A8 The sites, where smaller threshold levels are introduced.

Table A3 Threshold values for deforestation detection

	HV	HH	HH/HV
Area1	-2.5 dB	2.0 dB	1.5 dB

Area2	-2.5 dB	0.5 dB	1.5 dB
Area3	-2.5 dB	2.0 dB	0.5 dB
Area4	-2.5 dB	0.5 dB	0.5 dB
Area5	-1.5 dB	0.5 dB	0.5 dB
Area6	-1.5 dB	0.5 dB	1.5 dB
Area7	-1.5 dB	2.0 dB	0.5 dB
Area8	-1.5 dB	2.0 dB	1.5 dB

■ Algorithm Ver. 3.1

Despite the various major improvements in the Ver. 3 algorithm there are still some factors that drastically hamper the reliability of the produced forest warnings. Due to these prevailing issues with critically low deforestation detection accuracies of Ver. 3 algorithm, this update introduces a novel false alarm suppression method based on advanced time-series analysis using all available JJ-FAST PALSAR-2 ScanSAR data. Note that the basic change detection method for deforestation detection of Ver. 3 is unchanged. The processing flow for Ver 3.1 which is in use since March 7, 2022, is shown in Fig. A9. As most of the severely low accuracy results are related to flooding and rainfall effects, we propose a new full-resolution flood forest mask which can be used to filter out all false positives caused by heavy rain and flooding of forest floor. An example of such a flood forest map is shown in Fig. A10. The map is based on the full ALOS-2 time-series using 73 cycles. It is the first time that such a reliable high-resolution and area-wide flood forest information has been used and it well demonstrates the tremendous potential of the unprecedented ALOS-2/PALSAR-2 long-term observation archive. The filtering of error polygons is done on the basis of a proposed omega parameter. This parameter is calculated for every QL polygon by using the information form the flood forest masks. Omega parameter is calculated using the mean temporal standard deviation of all ScanSAR image pixels inside a given polygon and the maximum temporal standard deviation out of all the pixels inside the polygon (Fig. A11) as

$$\omega = \frac{\frac{2}{s}(\sum_{i=1}^{s} x_i) + \max_{i \in [s]} x_i}{3}$$

where s is the number of pixels inside the detected polygon and x_i is the γ^0 standard deviation of pixel i.

It has been confirmed that the new method can reduce the number of false positives by up to 97.5% depending on the severity of the rainfall events and flooding conditions.

In addition, in Ver 3.1 we introduce a new PALSAR-2 ScanSAR time-series FNF mask to drastically reduce false detections related to incorrect landcover information. The new forest mask is also based on the ScanSAR full time-series analysis. In principle, the decision whether an image pixel is covered by forest or not is made based the 5th percentile (*P5*) of the γ^0_{HV} time-series (Fig. A12). If a pixel exceeds a threshold value (e.g., -16.5 dB in the case of Amazon basin) it is classified as forest, and if it is below that threshold it is classified as non-forest. The new approach has several main advantages over the old forest mask. First, the maps are self-updating with every new cycle,

keeping them always up-to-date. Second, the masks are produced for every RPS path resulting in exactly matching image geometries. And lastly, the new maps are much more reliable than the older maps because the time-series approach largely reduces all uncertainties caused by spatial-temporal variability and seasonality effects which are one of main shortcomings of the classical single-temporal data based maps.

As it was confirmed that the TS-FNF has higher reliability than the National forest map products used in Brazil and Peru, these maps will no longer be used in the JJ-FAST, but instead only the new ScanSAR TS-FNF will be used in for entire Latin America in a more consistent fashion. It should be noted that this is the first update of the forest mask since introducing FNF 2017 edition in May 2018. Due to the far superior reliability of the new map, a significant reduction in error detections related to incorrect land cover information (e.g., crop land and pasture) is expected.

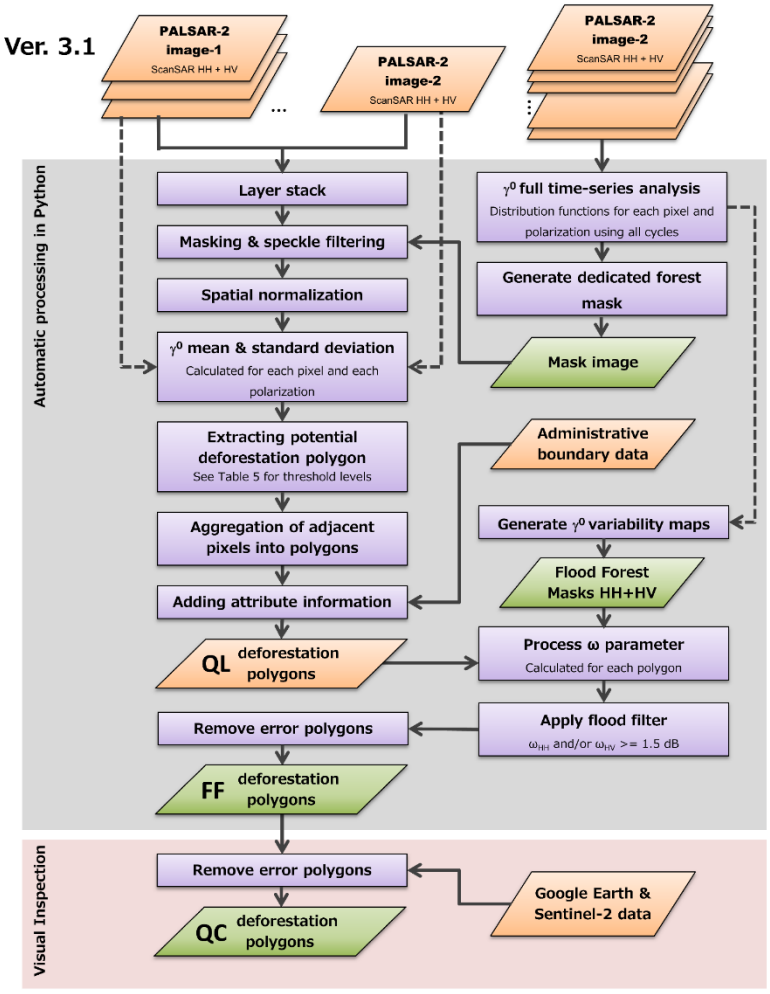

Fig. A9 Processing flow of deforestation detection algorithm Ver. 3.1.

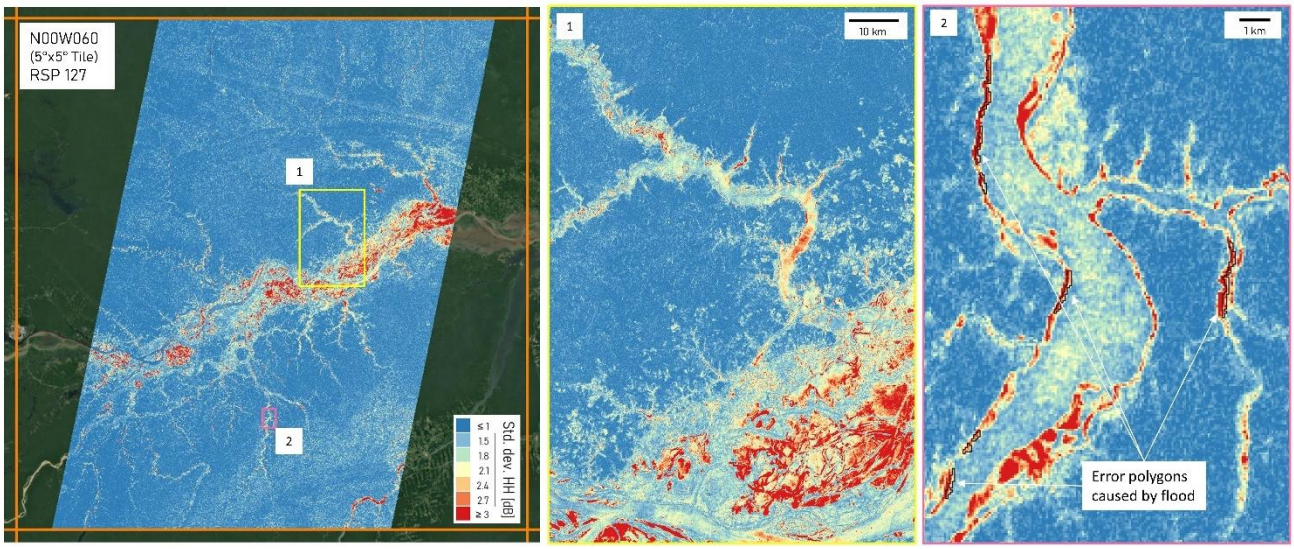

Fig. A10 New high-resolution flood forest mask based on ALOS-2/PALSAR-2 ScanSAR full time-series.

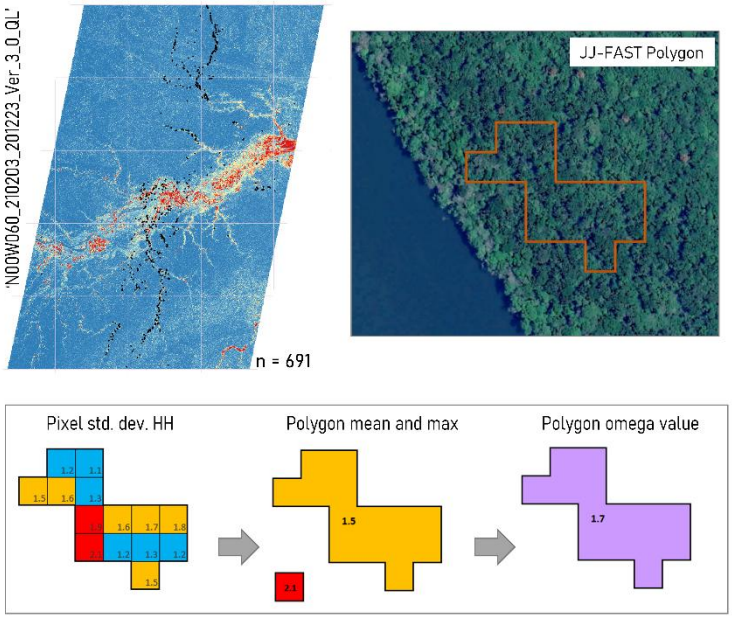

Fig. A11 Flood forest mask based false alarm suppression by omega parameter.

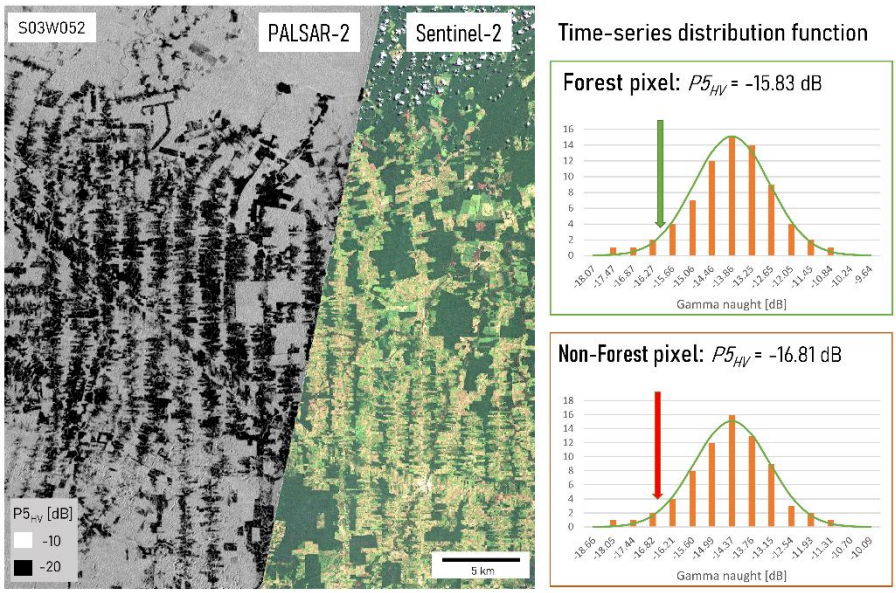

Fig. A12 Principle for full time-series based forest/non-forest classification.

■ Algorithm Ver. 3.2

Algorithm ver. 3.2 is the same processing procedure as Algorithm ver. 3.1. However, the basic processing software Sigma-SAR to generate the input PALSAR-2/ScanSAR image has been revised. This revision has improved the geolocation accuracy of PALSAR-2 image, and almost eliminated the shift between PALSAR-2 images at two different times, which was sometimes seen previously. As a result, error detections due to the shift has been substantially reduced. In addition, Ver. 3.2 is applied to the entire JJ-FAST target area, whereas Ver. 3.1 was applied only to Central and South America.

The Ver. 3.2 algorithm expands the use of the improved processing scheme, which Ver 3.1 previously introduced in Latin America only, to the entire JJ-FAST area. The advanced false alarm suppression and the new TS-FNF significantly improve the user's accuracy in both Africa and Southeast Asia. Moreover, the basic ScanSAR processing software Sigma-SAR was upgraded from v2.4.0 to v3.0.0. The new processor version greatly improves the geolocation accuracy of PALSAR-2 ScanSAR images. As a result, error detections caused by unstable image geometry (i.e., shifted image pixels) have been largely eliminated.

A2. Verification

■ Verification based on the ground survey

In four countries of Peru, Botswana, Gabon, and Brazil, we have so far performed the verification of accuracy based on the ground survey. As a result, it was verified that deforestation was correctly detected with reference to 19 polygons among 25 polygons. The accuracy of this system (User's Accuracy) is calculated to be 76.0%. These correct detection results represented logging areas for the development of farmlands and oil palm plantations. In contrast,

the erroneous detection results represented the falsely detected change in the vegetation of farmlands and grasslands.

■ **Verification based on the optical satellites data**

Ver. 3.0 algorithm were evaluated by the optical satellite data for 11 validation sites. The 11 test sites are selected from various forest type in Africa, middle and south America, and SE-Asia, and the characteristics are summarized in Table A4. Validation data was produced from Landsat based validation data (GLAD) and visually inspected Sentinel-2 data, and the evaluation results are presented in Table A5. User's and producer's accuracies are achieved to be 85.0%, and 62% in average for ver. 3 algorithm.

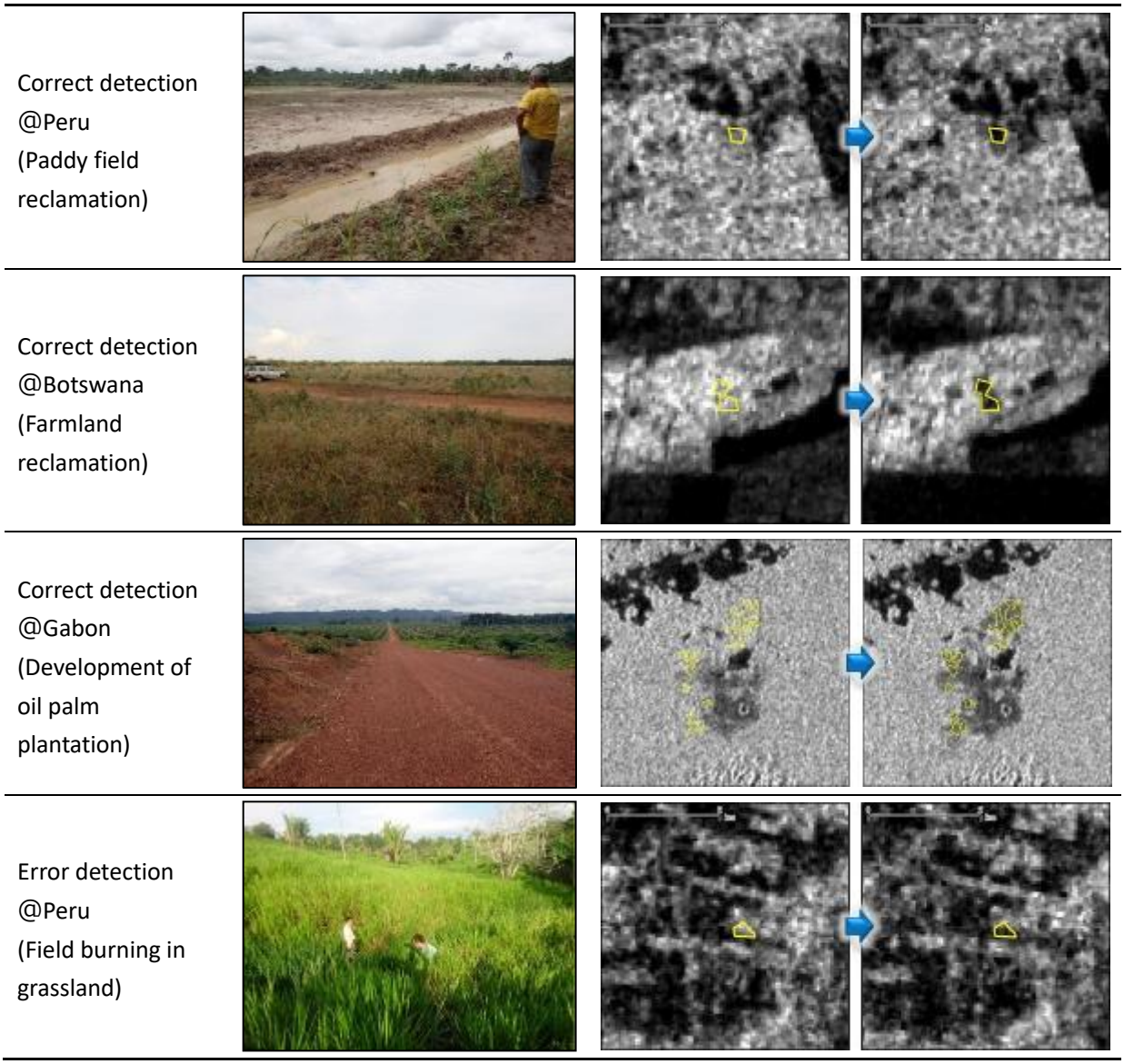

Fig. A13 Examples of the verification results of accuracy based on ground surveys

5. Two types of JJ-FAST products, QL and QC (discontinued)

Due to largely insufficient performance of the old algorithms , from 1 July, 2019, to 17 April 2023, JJ-FAST has been delivering two types of polygon products of Quick Look (QL) and Quality Checked (QC). QL products were available shortly after the ALOS-2 observations with a delay of only 3-4 days. Polygons distributed via the QL products contain all deforestations detected by the Old JJ-FAST algorithm. Note that the QL deforestation polygons are validated and therefore show significantly higher false alarm rates and low accuracy. The usual “Quality Checked” (QC) products with validated deforestation polygons will be released 4-7 days after the observations as always. The locations of the latest QL and QC detections are shown as purple and red pins on the JJ-FAST map, respectively. As before, the locations of all past deforestation detections will be shown as yellow pins.

User can select the QC or QL polygons by using the Data Select menu in which QL polygons can be identified by text “(QL)” in the list (Fig.15) and QC polygons are listed in observation term only (without (QL)).

The filename of QL products has a string “_QL” before extension (e.g. S10W062_190701_190422_02_QL.shp).

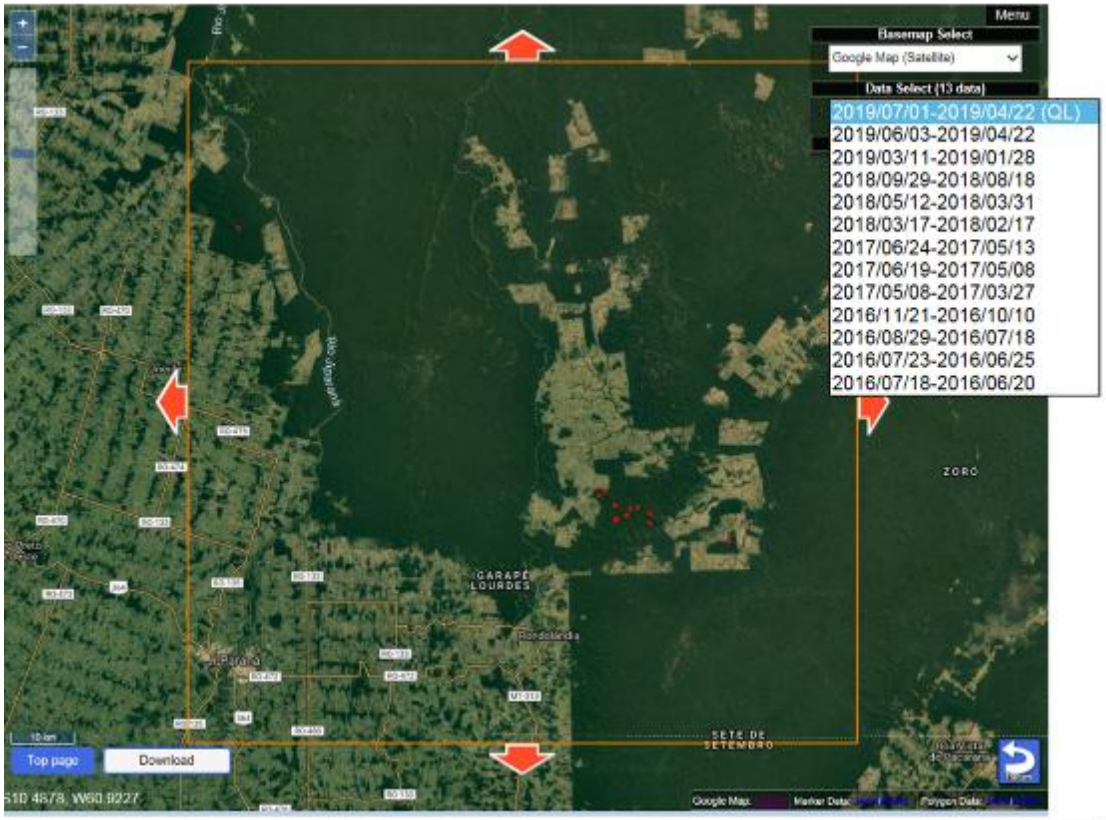

Fig. A14 Example of the Data Select

■ Points of caution when using JJ-FAST Quick Look (QL) products

Fig. 16 shows some examples of erroneously detected polygons by Ver. 3.0 deforestation detection algorithm. Fig. 16-a) shows a typical error polygon observed near a river. The flood occurred in a forest induces strong reflection in HH polarization and induces the error polygons by the algorithm with HH and HH/HV polarization. These error

polygons are found especially in JJ-FAST QL products generated with the Ver. 3.0. Note that these kind of flood and rainfall related errors have been largely eliminated by the advanced false alarm suppression methods introduced with Ver. 3.1. Fig. 16-b) is an example of error polygons observed in an agriculture area. After harvesting agricultural products induces weak reflection in HV polarization and induces the error polygons by the algorithm with HV polarization. Note that these kinds of errors also have been greatly reduced by introducing the new self-updating ScanSAR time-series based forest mask in Ver. 3.1. Fig. 16-c) is an example of error polygons observed in the mountain area. Bright (white) color in the image is called layover, which is unique for SAR image. This is made artificially in a hilly mountain area. The layover area is removed in the deforestation detection algorithm. But failure of the layover mask often induces the error detection by the algorithm with HH polarization.

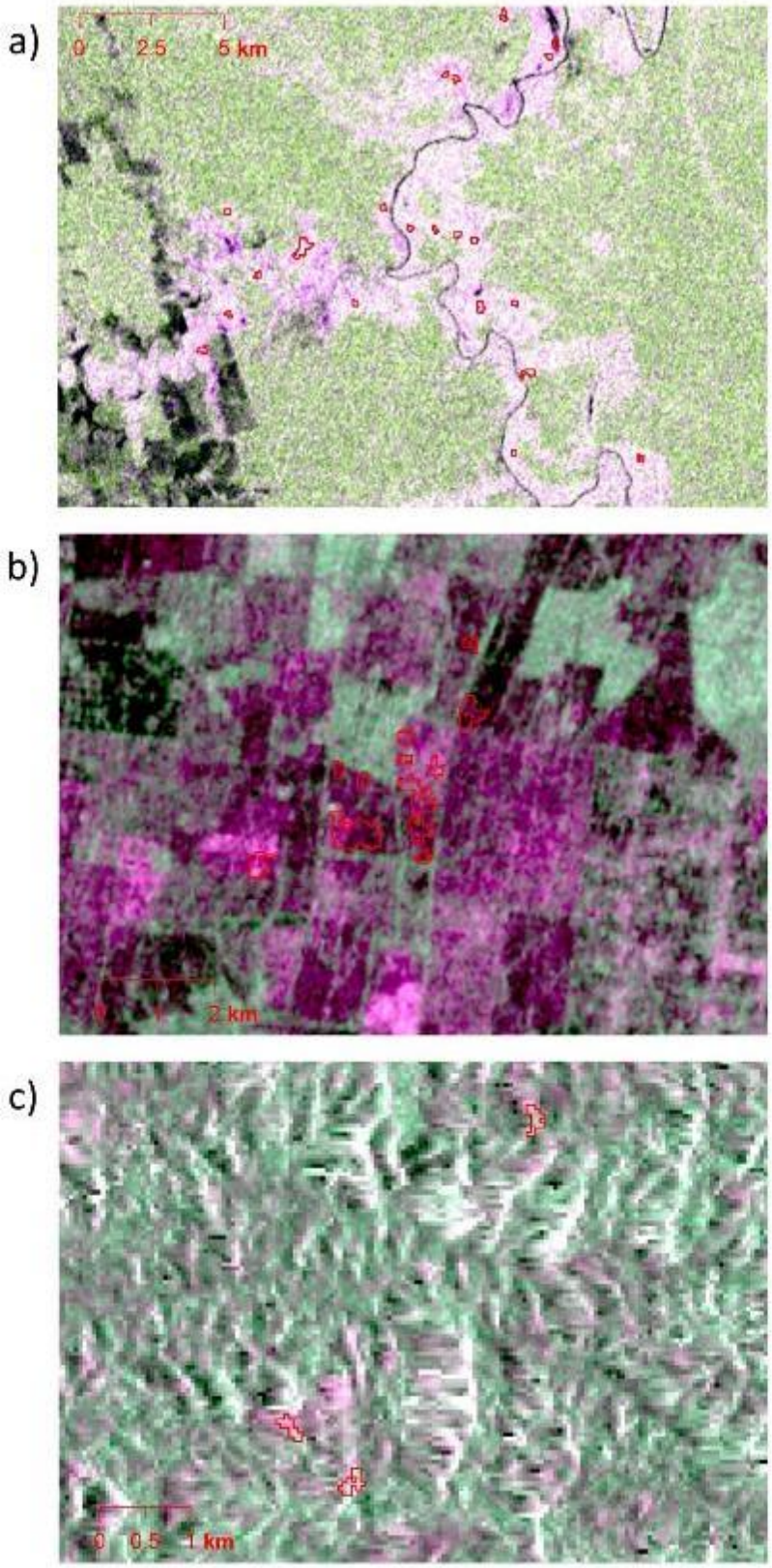

Fig. A15 Example of error detection. a) Observed near river. b) Observed in an agriculture area. c) Observed in the mountain area.

Table A4 Validation sites

Area	Country	1°x1°-Tile	Detection period	Characteristics
Africa	Mozambique	S16E036	191002_190821	Typical dry forest in Africa with scores of observed deforestations.
	DR Congo	S04E027	191009_190828	
	Cameroon	N07E014	190511_190330	
Middle-South America	Brazil	S03W052	191001_190820	Typical tropical forest deforestation site
	Guatemala	N15W092	190508_190327	Scores of deforestations observed in middle America
	Brazil	S13W049	190925_190814	Cerrado biome (tropical savanna) is dominant.
	Peru	S08W075	190824_190713	Typical tropical forest deforestation site
SE-Asia	Myanmar	N12E099	190509_190328	Scores of deforestations observed in the mountainous area.
	Indonesia	S02E102	191018_190823 190405_190322	Typical tropical forest deforestation site
	Vietnam	N12E106	191013_190901	Scores of deforestation observed (some plantation areas included)

Table A5 Deforestation detection accuracies for ver. 3 algorithm.

	Number of polygons			Accuracies (%)		
	Detected	Correct	Validation	User's	Producer’s	Overall
N07E014_190511	30	30	51	100	58.8	58.8
N12E099_190509	194	174	237	89.7	73.4	67.7
N12E106_191013	174	172	189	98.9	91.0	90.1
N15W092_190508	77	63	158	81.8	39.9	36.6
S02E102_190405	118	74	131	62.7	56.5	42.3
S02E102_191018	472	425	576	90.0	73.8	68.2
S03W052_191001	1142	629	964	55.1	65.3	42.6
S04E027_191009	184	183	208	99.5	88.0	87.6
S08W075_190824	520	363	614	69.8	59.1	47.1
S13W049_190925	69	60	74	87.0	81.1	72.3
S16E036_191002	50	50	325	100	15.4	15.4

Table A6 ALOS-2/PALSAR-2 ScanSAR data and algorithm version history

Observation cycle	Observation period	Applied Algorithm
45	2016.03.28 – 2016.04.10	Ver. 0.0
48	2016.05.09 – 2016.05.22	Ver. 0.0
51	2016.06.20 – 2016.07.03	Ver. 0.0
53	2016.07.18 – 2016.07.31	Ver. 0.0
56	2016.08.29 – 2016.09.11	Ver. 0.0
59	2016.10.10 – 2016.10.23	Ver. 0.0
62	2016.11.21 – 2016.12.04	Ver. 0.0
65	2017.01.02 – 2017.01.15	Ver. 0.0
68	2017.02.13 – 2017.02.26	Ver. 0.0
71	2017.03.27 – 2017.04.09	Ver. 0.0
74	2017.05.08 – 2017.05.21	Ver. 0.0
77	2017.06.19 – 2017.07.02	Ver. 0.0
79	2017.07.17 – 2017.07.30	Ver. 1.0
82	2017.08.28 – 2017.09.10	Ver. 1.0
85	2017.10.09 – 2017.10.22	Ver. 1.0
88	2017.11.20 – 2017.12.03	Ver. 1.0
91	2018.01.01 – 2018.01.14	Ver. 1.0
93	2018.01.29 – 2018.02.11	Ver. 1.0
94	2018.02.12 – 2018.02.25	Ver. 1.0
96	2018.03.12 – 2018.03.25	Ver. 1.0
97	2018.03.26 – 2018.04.08	Ver. 1.0
99	2018.04.23 – 2018.05.06	Ver. 2.0
100	2018.05.07 - 2018.05.20	Ver. 2.0
102	2018.06.04 – 2018.06.17	Ver. 2.0
103	2018.06.18 – 2018.07.01	Ver. 2.0
104	2018.07.02 – 2018.07.15	Ver. 2.0
105	2018.07.16 – 2018.07.29	Ver. 2.0
107	2018.08.13 – 2018.08.26	Ver. 2.0
108	2018.08.27 – 2018.09.09	Ver. 2.0
110	2018.09.24 – 2018.10.07	Ver. 2.0
111	2018.10.08 – 2018.10.21	Ver. 2.0
113	2018.11.05 – 2018.11.18	Ver. 2.0
114	2018.11.19 – 2018.12.02	Ver. 2.0
116	2018.12.17 – 2018.12.30	Ver. 2.0
117	2018.12.31 – 2019.01.13	Ver. 2.0
119	2019.01.28 – 2019.02.10	Ver. 2.0
120	2019.02.11 – 2019.02.24	Ver. 2.0
122	2019.03.11 – 2019.03.24	Ver. 2.0
123	2019.03.25 – 2019.04.07	Ver. 2.0
125	2019.04.22 – 2019.05.05	Ver. 2.0
126	2019.05.06 – 2019.05.19	Ver. 2.0
128	2019.06.03 – 2019.06.16	Ver. 2.0
129	2019.06.17 – 2019.06.30	Ver. 2.0
130	2019.07.01 – 2019.07.14	Ver. 2.1
131	2019.07.15 – 2019.07.28	Ver. 2.1
133	2019.08.12 – 2019.08.25	Ver. 2.1
134	2019.08.26 – 2019.09.08	Ver. 2.1
136	2019.09.23 – 2019.10.06	Ver. 2.1
137	2019.10.07 – 2019.10.20	Ver. 2.1
139	2019.11.04 – 2019.11.17	Ver. 2.1
140	2019.11.18 – 2019.12.01	Ver. 2.1
142	2019.12.16 – 2019.12.29	Ver. 2.1
143	2019.12.30 – 2020.01.12	Ver. 2.1
145	2020.01.27 – 2020.02.09	Ver. 2.1
146	2020.02.10 – 2020.02.23	Ver. 2.1
148	2020.03.09 – 2020.03.22	Ver. 2.1
149	2020.03.23 – 2020.04.05	Ver. 2.1
151	2020.04.20 – 2020.05.03	Ver. 2.1
152	2020.05.04 – 2020.05.17	Ver. 2.1

154	2020.06.01 – 2020.06.14	Ver. 3.0
155	2020.06.15 – 2020.06.28	Ver. 3.0
156	2020.06.29 – 2020.07.12	Ver. 3.0
157	2020.07.13 – 2020.07.26	Ver. 3.0
158	2020.07.27 - -2020.08.09	Ver. 3.0
159	2020.08.10 – 2020.08.23	Ver. 3.0
160	2020.08.24 – 2020.09.06	Ver. 3.0
162	2020.09.21 – 2020.10.04	Ver. 3.0
163	2020.10.05 – 2020.10.18	Ver. 3.0
165	2020.11.02 – 2020.11.15	Ver. 3.0
166	2020.11.16 – 2020.11.29	Ver. 3.0
168	2020.12.14 – 2020.12.27	Ver. 3.0
169	2020.12.28 – 2021.01.10	Ver. 3.0
171	2021.01.25 – 2021.02.07	Ver. 3.0
172	2021.02.08 – 2021.02.21	Ver. 3.0
174	2021.03.08 – 2021.03.21	Ver. 3.0
175	2021.03.22 – 2021.04.04	Ver. 3.0
177	2021.04.19 – 2021.05.02	Ver. 3.0
178	2021.05.03 – 2021.05.16	Ver. 3.0
180	2021.05.31 – 2021.06.13	Ver. 3.0
181	2021.06.14 – 2021.06.27	Ver. 3.0
182	2021.06.28 – 2021.07.11	Ver. 3.0
183	2021.07.12 – 2021.07.25	Ver. 3.0
185	2021.08.09 – 2021.08.22	Ver. 3.0
186	2021.08.23 – 2021.09.05	Ver. 3.0
188	2021.09.20 – 2021.10.03	Ver. 3.0
189	2021.10.04 – 2021.10.17	Ver. 3.0
191	2021.11.01 – 2021.11.14	Ver. 3.0
192	2021.11.15 – 2021.11.28	Ver. 3.0
194	2021.12.13 – 2021.12.26	Ver. 3.0
195	2021.12.27 – 2022.01.09	Ver. 3.0
197	2022.01.24 – 2022.02.06	Ver. 3.0
198	2022.02.07 – 2022.02.20	Ver. 3.0
200	2022.03.07 – 2022.03.20	Ver. 3.1, Ver 3.0[1)]
201	2022.03.21 – 2022.04.03	Ver. 3.1, Ver 3.0[1)]
203	2022.04.18 – 2022.05.01	Ver. 3.1, Ver 3.0[1)]
204	2022.05.02 – 2022.05.15	Ver. 3.1, Ver 3.0[1)]
206	2022.05.30 – 2022.06.12	Ver. 3.1, Ver 3.0[1)]
207	2022.06.13 – 2022.06.26	Ver. 3.1, Ver 3.0[1)]
208	2022.06.27 – 2022.07.10	Ver. 3.1, Ver 3.0[1)]
209	2022.07.11 – 2022.07.24	Ver. 3.1, Ver 3.0[1)]
211	2022.08.08 – 2022.08.21	Ver. 3.1, Ver 3.0[1)]
212	2022.08.22 – 2022.09.04	Ver. 3.1, Ver 3.0[1)]
214	2022.09.19 – 2022.10.02	Ver. 3.2
215	2022.10.03 – 2022.10.16	Ver. 3.2
217	2022.10.31 – 2022.11.13	Ver. 3.2
218	2022.11.14 – 2022.11.27	Ver. 3.2
220	2022.12.12 – 2022.12.25	Ver. 3.2
221	2022.12.26 – 2023.01.08	Ver. 3.2
223	2023.01.23 – 2023.02.05	Ver. 3.2
224	2023.02.06 – 2023.02.19	Ver. 3.2
226	2023.03.06 – 2023.03.19	Ver. 3.2
229	2023.04.17– 2023.05.01	Ver. 4.0
230	2023.05.01 - 2023.05.14	Ver. 4.0
232	2023.05.29 - 2023.06.11	Ver. 4.0
233	2023.06.12 - 2023.06.25	Ver. 4.0
234	2023.06.26 - 2023.07.09	Ver. 4.0
235	2023.07.10 - 2023.07.23	Ver. 4.0
237	2023.08.07 - 2023.08.20	Ver. 4.0
238	2023.08.21 - 2023.09.03	Ver. 4.0
240	2023.09.18 - 2023.10.01	Ver. 4.0
241	2023.10.02 - 2023.10.15	Ver. 4.0
243	2023.10.30 - 2023.11.12	Ver. 4.1

244	2023.11.13 - 2023.11.26	Ver. 4.1
246	2023.12.11 - 2023.12.24	Ver. 4.1
247	2023.12.25 - 2024.01.07	Ver. 4.1
249	2024.01.22 - 2024.02.04	Ver. 4.1
250	2024.02.05 - 2024.02.18	Ver. 4.1
252	2024.03.04 - 2024.03.17	Ver. 4.1
253	2024.03.18 - 2024.03.31	Ver. 4.1
255	2024.04.15 - 2024.04.28	Ver. 4.1
256	2024.04.29 - 2024.05.12	Ver. 4.1
258	2024.05.27 - 2024.06.09	Ver. 4.1
259	2024.06.10 - 2024.06.23	Ver. 4.1
260	2024.06.24 - 2024.07.07	Ver. 4.1
261	2024.07.08 - 2024.07.21	Ver. 4.1
263	2024.08.05 - 2024.08.18	Ver. 4.1
264	2024.08.19 - 2024.09.01	Ver. 4.1
266	2024.09.16 - 2024.09.29	Ver. 4.1
267	2024.09.30 - 2024.10.13	Ver. 4.1
270	2024.11.11 - 2024.11.24	Ver. 4.1
271	2024.11.25 - 2024.12.08	Ver. 4.1
272	2024.12.09 - 2024.12.22	Ver. 4.1
273	2024.12.23 - 2025.01.05	Ver. 4.1
275	2025.01.20 - 2025.02.02	Ver. 4.1
276	2025.02.03 - 2025.02.16	Ver. 4.1
278	2025.03.03 - 2025.03.16	Ver. 4.1
279	2025.03.17 - 2025.03.30	Ver. 4.1
281	2025.04.14 - 2025.04.27	Ver. 4.1
282	2025.04.28 - 2025.05.11	Ver. 4.1
284	2025.05.26 - 2025.06.08	Ver. 4.1
285	2025.06.09 - 2025.06.22	Ver. 4.1
286	2025.06.23 - 2025.07.06	Ver. 4.1
287	2025.07.07 - 2025.07.20	Ver. 4.1
289	2025.08.04 - 2025.08.17	Ver. 4.1
290	2025.08.18 - 2025.08.31	Ver. 4.1
292	2025.09.15 - 2025.09.28	Ver. 4.1
293	2025.09.29 - 2025.10.12	Ver. 4.1
296	2025.11.10 - 2025.11.23	Ver. 4.1
297	2025.11.24 - 2025.12.07	Ver. 4.1
298	2025.12.08 - 2025.12.21	Ver. 4.1
299	2025.12.22 - 2026.01.04	Ver. 4.1
301	2026.01.19 - 2026.02.01	Ver. 4.1
302	2026.02.02 - 2026.02.15	Ver. 4.1
304	2026.03.02 - 2026.03.15	Ver. 4.1
305	2026.03.16 - 2026.03.29	Ver. 4.1
307	2026.04.13 - 2026.04.26	Ver. 4.2

[1)] Ver. 3.1 was used in Latin America and Ver. 3.0 is used in Africa, Asia, and Oceania.

Table A7 Ancillary data

Data type	Data source	ALOS-2 cycles	Geographic region
Forest map	ALOS/PALSAR forest/non-forest (FNF) map 2010 edition	45 – 82	Global
	ALOS-2/PALSAR-2 FNF map 2016 edition	85 – 99	Global
	ALOS-2/PALSAR-2 FNF map 2017 edition	100 –	Global
	ALOS-2/PALSAR-2 ScanSAR time-series FNF map 2021 edition	200 –	Latin America
	ALOS-2/PALSAR-2 flood forest map 2021 edition	200 –	Latin America
	GeoBosques forest and non-forest maps 2014 edition	85 – 99	Peru
	GeoBosques forest and non-forest maps 2016 edition	100 –	Peru
	DFRR/JICA Botswana Forest Distribution Map	85 –	Botswana
	PRODES forest and non-forest maps 2017 edition	91 –	Brazil
Topography	Shuttle Radar Topography Mission (SRTM) – 3	45 – 229	Global
	ALOS World 3D (AW3D30) DEM	235 –	Global
Urban area map	Global Human Settlement Layer (GHSL) 2014 edition	111 –	Global
Administrative borders	Database of Global Administrative Areas (GADM) ver. 2.8	45 – 99	Global
	Database of Global Administrative Areas (GADM) ver. 3.6	100 –	Global
Forest biomass map	LUCID Land use, carbon & emission data 2019 edition	126 –	Global

Table A8 JSON data structure

keys					descreption
{					
file_name:					Filename without extension
"product":					JFP for JJ-FAST Products
	"source_data": {				
		"S00": {			Ortho-rectified and slope corrected image product ID
			"file_name":		filename
			"product":		"Tile" for 1x1 grid tile or "Tile_5x5" for 5x5 grid tile.
			"obs_date":		Date of observation
			"polarization":		polarization
			"rsp":		Orbital pass number of Reference System for Planning (RSP)
			"cycle":		Observation cycle number
			"obs_mode":		"WBD" observation mode
			"off-nadir_angle":		Off nadir angle (degree)
			"satellite_direction":		"A", ascending / "D", descending
			"look_side":		"R", right / "L", left
			"replay_id":		
			"version":		Version of image product
			"DEM":		Type of Digital Elevation Model, Shuttle Radar Topography Mission (SRTM1)
			"upper_left_latitude":		Latitude of Upper Left pixel
			"upper_left_longitude":		Longitude of Upper Left pixel
			"pixel":		Number of columns in pixel
			"line":		Number of rows in pixel
			"Credit":		Crediting
		}			
	}				
	"polygon_info": {				
		"method":			An identifier that distinguishes between manual and automatic process. "MANUAL" is the current process with visual interpretation. "AUTO" is a fully automated process without any visual interpretation.
		"version":			Polygon version according to programs, input-files, parameters, etc.
		"P0001": {			
			"Country":		Country name where the polygon center is located
			"Continent":		Continent name where the polygon center is located
			"ChangeArea":		Area of polygon in hectares
			"Accuracy":		Reliability of detection results, 1 : high reliability / 2 : medium reliabilty
			"Polygon_id":		ID for identifying each polygon
			"State":		State name where the polygon center is located
			"Town":		Town name where the polygon center is located
			"Latitude":		Latitude of the polygon center
			"Longitude":		Longitude of the polygon center
			"Algorithm":		Methodology of deforestation detection
			"AlgoVer":		Version of algorithm
			"Threshold":		Threshold area defined for version 3 algorithm
			"CONTENTS":		"Deforestation"
		}			
	}				
"Credit":					Crediting
}					